Table 1 Patients' characteristics

Patient ID	Age/Sex	Stage	Meta site	MSKCC	Histology	Grade	Prior treatment
1802	72/F	pT3aN2M1	Lung, LN	Poor	Clear cell	2 > 3	Sunitinib
1803	72/M	pT3bN0M1	Liver, lung, bone	Poor	Clear cell	3 > 2	IFN-α, radiation
1806	72/F	pT4N1M1	Lung, LN	Intermediate	Clear cell	3	no
1808	75/M	pT3aN2M1	Lung, LN, bone	Intermediate	Unclassified	3	no
1812	61/M	pT1bN1M1	LN	Intermediate	Clear cell	2 > 1> > 3	no
1814	55/M	pT3aN0M1	Lung	Intermediate	Clear cell	2	no
1817	64/F	pT3bN1M1	Lung, LN, bone	Intermediate	Clear cell	3 > 2	no
1823	57/M	pT1N0M1	Lung, pleura	Intermediate	Clear cell	2 > 3	no

MSKCC, Memorial Sloan Kettering Cancer Center risk criteria; LN, lymph node.

after sunitinib treatment) ($p = 0.23$, Wilcoxon signed-rank test). For Tregs, the percentages of $CD25^+Foxp3^+$ cells within the $Dye450^-CD3^+CD4^+$ population (Additional file 3) were found to be decreased relative to the baseline in patients #1802, #1803 and #1814, but not in patients #1806, #1808, #1812, #1817 and #1823 (Figure 2B). However, there was no statistical difference ($p = 0.273$, Wilcoxon signed-rank test).

DTH reactions and tumor-reactive T cell responses

DTH testing was performed in all 8 patients to detect tumor lysate-reactive responses. Three patients (#1802, #1814 and #1823) had positive DTH reactions (Table 4). Tumor lysate-reactive $CD4^+$ and $CD8^+$ T cell responses in all patients were further investigated in vitro using the IFN-γ secretion assay at different time points after vaccination. Data from an individual patient #1802 are shown in Additional file 3. Before vaccination, the percentage of $CD8^+$ IFN-γ^+ T cells after simulation with EP-DCs or unloaded DCs was essentially identical (1.6%-vs-1.4%, respectively). However, after vaccination, a higher percentage of $CD8^+$ IFN-γ^+ T cells was observed on stimulation with EP-DCs (2.9%) than with unloaded DCs (1.5%). Similarly, a higher percentage of $CD4^+$ IFN-γ^+ T cells was observed on stimulation with EP-DCs (4.5%) than with unloaded DCs (3.0%). These T cell responses fluctuated during the course of treatment and no statistically significant difference in the increase of IFN-γ^+ T cells after vaccination was detected. Figure 2C shows the percentage of tumor lysate-reactive IFN-γ^+ cells (both $CD4^+$ as well as $CD8^+$ T cells) for all 8 patients. When the percentages at any point after vaccination are elevated 3-fold higher than those at the baseline (mean value of the percentages at days 0 and 14), the tumor-reactive T cell responses are considered to be positive. By this criteria, the induction of tumor lysate-reactive $CD4^+$ T cell responses were detected in patients #1802, #1803, #1814 and #1823; patients #1802, #1812, #1814 and #1823 had tumor-reactive $CD8^+$ T cell responses (Table 4). The T cell responses were detected even at the time of registration in Patients #1808 and 1812.

Concentration of IL-8 in the sera

To search for biomarkers predicting responsiveness to combination therapy with sunitinib and DC-based immunotherapy, we analyzed concentrations of IFN-γ, IL-1β, IL-2, IL-4, IL-5, IL-6, IL-8, IL-10, IL-12 p70, TNF-α, and TNF-β in sera from the 8 patients before and during treatment. With the exception of IL-8, which was present at different levels in all patients, serum cytokines were barely detectable. Patients #1806, #1808, #1817 and #1823 had greatly elevated levels of >60 pg/ml IL-8 during treatment (Figure 2D and Table 4), whereas patients #1802, #1803, #1812, and #1814 had basal levels <60 pg/ml.

Table 2 Quality and quantity of tumor lysate-loaded DCs

Patient ID	Tumor lysate used for EP (mg)	DCs used for EP (x10^7)	Tumor lysate (mg)/ 10^7 DCs	Number of DCs injected	Viability (%)
1802	15	29.5	0.51	1x10^7	82.9
1803	15	18.3	0.82	1x10^7	82.1
1806	20	17.1	1.17	1x10^7	92.8
1808	7	16.0	0.44	1x10^7	83.6
1812	20	20.1	1.00	1x10^7	89.0
1814	20	21.5	0.93	1x10^7	91.7
1817	20	20.0	1.00	1x10^7	87.5
1823	20	15.0	1.33	0.5 x10^7	92.4

EP, electroporation.

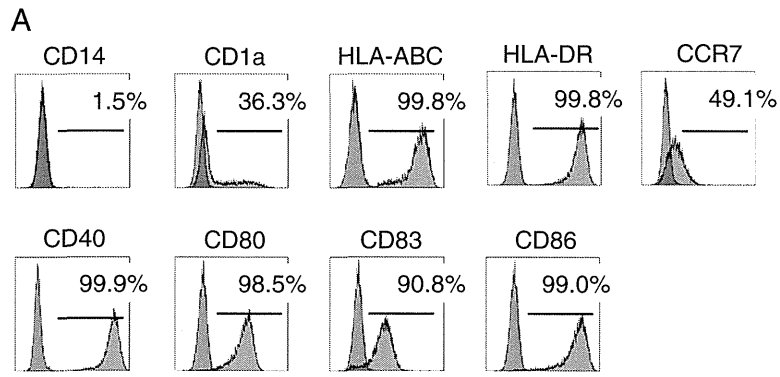

Figure 1 Surface phenotype of DCs; specific mAb staining (red) and isotype control mAb staining (blue).

Clinical responses

The follow-up period ranged from 100 to 1140 days (Table 4). Except for one patient who died of a brain hemorrhage due to hypertension, patients remained alive during the trial with a median overall survival (OS) of 346 days and median progression-free survival (PFS) of 164 days. One patient achieved a complete response (CR), another patient had a partial response (PR), 3 had stable disease (SD) and 2 had progressive disease (PD) according to the RECIST criteria (Table 4). Patient #1814 who achieved the CR was one of three patients who had developed DTH, as well as $CD4^+$ and $CD8^+$ T cell responses. In this patient, the percentages of both MDSCs and Tregs decreased during treatment. In the CT scan, the size of the mass in the left lung decreased from 17.9 mm to 8.2 mm in diameter after 6 immunizations and had disappeared after 10 (Additional file 4). The other patient who had a DTH reaction, #1802, also had $CD4^+$ and $CD8^+$ T cell responses, as well as decreased MDSCs and Tregs, and low IL-8. She manifested SD in spite of multiple tumor metastases in the lung (Additional file 4). Her quality of life was markedly improved by a reduction of the pleural effusion (Additional file 4). As shown in Additional file 4, the tumor volume was decreased and pleural effusion was reduced in patient #1823, who develop also positive DTH, $CD4^+$ and $CD8^+$ T cell responses (Table 4). Patient #1812 was defined as PD when target lesion, supraclavicular lymph node metastasis, was enlarged by 30.3% in size. Therefore, he received surgery to resect the metastatic lymph node and no recurrence was observed with no further treatment.

Safety

The most common adverse events were hand-foot syndrome, stomatitis, peripheral edema and other skin disorders (Table 5). Sunitinib-related severe adverse events were hypertension and hematological and laboratory abnormalities. They were managed with interruption of sunitinib and were reversible in most cases, except for a fatal hypertensive intracranial hemorrhage in patient #1806 who had no brain metastasis. No severe adverse events related to DC therapy were observed.

Discussion

Here we report a clinical trial of DC-based immunotherapy combined with sunitinib in mRCC patients. We evaluated the safety and feasibility of this approach. In the course of treatment, one patient developed cerebral hemorrhage due to hypertension. However, no severe vaccination-related toxicity or autoimmunity was observed in any of the 8

Table 3 The surface phenotype of DCs

Patient ID	% Expression								
	CD14	CD1a	HLA-ABC	HLA-DR	CCR7	CD40	CD80	CD83	CD86
1802	7.8	51.6	98.7	99.7	10.6	99.9	96.4	60.1	96.3
1803	1.4	79.6	99.2	99.9	38.7	99.4	99.1	94.1	99.5
1806	1.5	36.3	99.8	99.8	49.1	99.9	98.5	90.8	99
1808	5.2	53.3	98.8	99.5	43.1	99.4	96.7	75.6	98.7
1812	0.6	83	99.9	99.7	10.3	99.8	99.2	87.4	97.9
1814	0.6	66.5	99.4	99.4	58.3	99.6	98.7	91.5	99.2
1817	1.4	34.7	99.7	98.3	50.3	99.8	96.7	61.8	98
1823	0.8	50.4	99.7	99.6	30.5	99.7	99.3	95.4	99.3

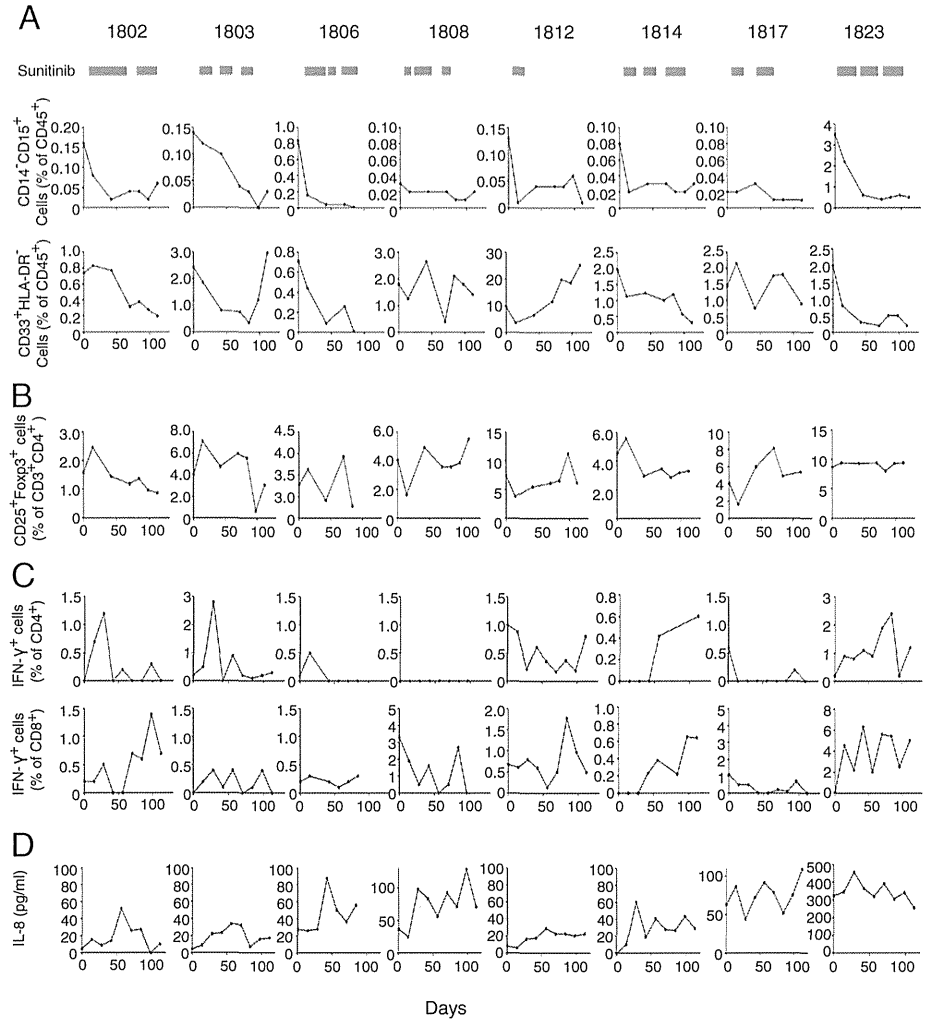

Figure 2 Immunomonitoring. A. Percentages of MDSCs by two criteria. **B**. Percentages of Tregs. **C**. Changes of tumor-reactive IFN-γ$^+$ cells (% of CD4$^+$ or CD8$^+$ T cells). Assay was performed as described in Methods section. **D**. The concentration of IL-8 in sera measured by a cytofluorometry-based ELISA system at different time points during treatment of the 8 patients.

patients treated. Sunitinib decreased the frequencies of peripheral blood MDSCs and/or Tregs. Vaccination with tumor lysate-loaded DCs induced tumor-reactive CD4$^+$ and/or CD8$^+$ T cell responses. The treatment showed some clinical benefits in patients possibly linked to successful control of immunosuppressive cells and induction of T cell responses. This was particularly notable in patient #1814 where lung metastases disappeared. However, there is a possibility that these clinical responses are solely due to sunitinib rather than vaccine-induced immune response, since the DC was given concurrently with sunitinib which is an active drug for the treatment of RCC.

Consistent with previous reports [27,29], we observed reduced percentages of MDSCs during sunitinib treatment, but only in 5 of 8 patients (Figure 2A and Table 4). Of these 5, 4 developed increased tumor-reactive T cell responses. However, the very low number of patients included in this study and the fluctuations in magnitude of T cell responses during the course of treatment make it difficult to conclude the relationship between MDSC and T cell responses. Regarding mechanisms underlying the modulation of MDSCs by sunitinib, it has been shown that this agent inhibits STAT3 signaling. This induces apoptosis in murine MDSCs, where STAT3 is a critical factor responsible for their expansion [31,32]. On the other hand, GM-CSF accumulating in the tumor expands MDSCs to promote sunitinib-resistance due to preferential STAT5 activation, which cannot be suppressed by sunitinib [33]. Thus, to understand the different sensitivity of MDSCs to sunitinib in different mRCC patients, the STAT3 or STAT5 activation status in the MDSCs and expression of cytokines such as GM-CSF in the tumor would need to be investigated.

A decreased percentage of Tregs after sunitinib treatment was also observed, although only in 3 of the 8

Table 4 Immune responses and clinical outcomes in 8 patients

ID	No. DC injection	DTH	CD4 T cell response	CD8 T cell response	MDSCs*	Tregs*	IL-8[†]	Change in Target Lesions (%)	Clinical Response[‡]	PFS[§](d)	OS[§](d)	Prognosis
1802	6	+	+	+	decreased	decreased	low	−25.4	SD	173	339	Dead
1803	6	-	+	-	decreased	decreased	low	0	SD	200	353	Dead
1806	6	-	-	-	decreased	no change	high	−18.4	N.A.[¶]	100	100	Dead
1808	6	-	-	-	no change	increased	high	−5.4	SD	155	193	Dead
1812	6	-	-	+	no change	no change	low	30.3	PD[#]	101	1140[‖]	Alive
1814	12	+	+	+	decreased	decreased	low	−100	CR	347	1127[‖]	Alive
1817	6	-	-	-	no change	increased	high	−27.8	PD[**]	88	206	Dead
1823	12	+	+	+	decreased	no change	high	−35.3	PR	342[‖]	342[‖]	Alive

PFS, progression free survival; OS, overall survival; CR, complete response; PR, partial response; SD, stable disease; PD, progressive disease.
*Compared to the baseline.
[†]High or low is defined as more or less than 60 pg/ml in sera.
[‡]4wks after last injection.
[§]From the registration (days).
[¶]Withdrawn from the study by sudden hypertensive cerebral hemorrhage.
[‖]A censored case due to the termination of the study.
[#]After surgical removal of target lesion (LN metastasis), no recurrence was observed.
[**]Though target lesion became smaller, accumulation of pleural effusion was increased.

patients (Figure 2B and Table 4). The mechanism underlying regulation of Tregs by sunitinib remains unclear. It has been proposed that the reduction of Tregs by sunitinib may be an indirect effect of the downregulation of MDSCs and/or increases in IFN-γ production [27]. In our case, reduced frequencies of Tregs were observed in 3 of the 5 patients who did show reduced MDSCs. No reduction of Tregs was seen in a further 3 of 3 patients in whom there was no reduction of MDSCs. Nevertheless, the number of patients was too small to lead to any conclusion.

To identify biomarkers for predicting outcome of combination sunitinib and DC-based immunotherapy, we tested a wide range of cytokines (IFN-γ, IL-1β, IL-2, IL-4, IL-5, IL-6, IL-8, IL-10, IL-12 p70, TNF-α, and TNF-β) in sera from patients before and during treatment. We found IL-8 in all patients, with 4 having highly elevated levels (>60 pg/ml) during treatment. IL-8 is a member of the CXC family of chemokines and is a potent proangiogenic factor [34]. Renal cell carcinoma has been shown to produce IL-8, and IL-8 expression is known to cause mRCC resistance to sunitinib [35,36]. IL-8 angiogenic signaling is thought to functionally compensate for the inhibition of VEGF/VEGFR-mediated angiogenesis. Further, the secretion of IL-8 from cancer cells may have a variety of effects on the tumor microenvironment, because the IL-8 receptors CXCR1 and CXCR2 are expressed on cancer cells, endothelial cells, neutrophils and tumor-associated macrophages. It has been shown that production of IL-8 by tumors induces Treg migration into tumors [36]. IL-8 produced by tumor cells may also recruit MDSCs into tumor sites. Therefore, high IL-8 expression may contribute to shaping the immunosuppressive environment in the tumor and inhibiting tumor-reactive T cell responses. In this study, no reduction of IL-8 was achieved by sunitinib (Figure 2D). Therefore, targeting IL-8 signaling may be required for improving this cancer vaccine.

Cancer immunotherapy based on the regulation of immunosuppressive cells, soluble factors, and signaling pathways are now considered essential element of the treatment of cancer [37]. Similar effects are also achieved by molecular targeted therapy, which primarily aims to inhibit molecular pathways that are crucial for tumor cell growth and survival. Importantly, such small molecule inhibitors may also modulate the immune system, which raises the possibility that targeted therapy might be effectively combined with immunotherapy to improve clinical outcomes [38]. This may indeed be the case in our small pilot study. A reduction of immunosuppressive cells by sunitinib likely contributed to stimulating anti-tumor immune responses induced by tumor lysate-loaded DC vaccines.

Initially 15 patients were planned to be included in this study; we terminate the study with 8 patients reproted here, because other TKIs, pazopanib and axitinib, and mTOR inhibitors, temsirolimus and everolimus, are now available for the RCC treatment in addition to sunitinib and sorafenib. A new pilot study is currently underway to determine the better combination of these molecular target drugs with DC-based immunotherapy. Though our

Table 5 Adverse Events and Laboratory abnormalities

	Grade					
Adverse Events, Regardless of Causality	All	1	2	3	4	5
General disorders						
Fatigue	2		2			
Pyrexia	2	1	1			
Insomnia	1		1			
Gastrointestinal disorders						
Dyspepsia	2		2			
Dysgeusia	2	1	1			
Diarrhea	2	2				
Nausea	1	1				
Esophagitis	1	1				
Respiratory, thoracic and mediastinal disorders						
Cough	1		1			
Musculoskeletal and connective tissue disorders						
Back pain	3	1	2			
Metabolism and nutrition disorders						
Hypothyroidism	4		4			
Skin and subcutaneous tissue disorders						
Hand-foot syndrome	8	2	6			
Stomatitis	4	2	2			
Peripheral Edema	4	3	1			
Anal diseases	3		3			
Skin ulceration	1		1			
Pruritus	1		1			
Trichophytosis	1		1			
Rash	1	1				
Vascular disorders						
Hypertension	3		1	1		1*
Hematological and other laboratory abnormalities						
Anemia	3		1	2		
Leukopenia	3			3		
Neutropenia	3			3		
Lymphocytopenia	3			3		
Thrombocytopenia	3			3		
Increased creatinine	2			2		

*Intracranial hemorrhage.

study has some limitations in that this is a single institution study and sample size was only 8 patients, our results support the notion that immunotargeted therapy represents an appropriate future direction for developing successful treatment of mRCC.

Conclusions

This pilot study of DC-based therapy together with sunitinib for mRCC patients has documented the safety and feasibility of this approach. The reduction of both MDSCs and Tregs was achieved by sunitinib in patients whose serum IL-8 levels were not excessive. Autologous tumor lysate-loaded DCs in combination with sunitinib induced both $CD4^+$ and $CD8^+$ T cell responses in mRCC patients.

Methods

Patient selection

A pilot study of DC-based immunotherapy combined with sunitinib in mRCC patients was conducted. The primary endpoints were the safety and feasibility of this approach; the secondary endpoints were to obtain immunological proof of concept and preliminary data for anti-tumor effect, overall survival (OS) and progression-free survival (PFS). Patients aged ≥20 years with advanced or recurrent mRCC who underwent nephrectomy were eligible for this clinical study of DC therapy combined with sunitinib. To be included, patients had to have an Eastern Cooperative Oncology Group performance status (PS) of 0, 1 or 2, normal kidney, liver, and bone marrow function, and at least 1 measurable cancer lesion assessed by computed tomography. Patients positive for anti-adult T-cell leukemia-associated antigen or anti-human immunodeficiency virus antibody, other primary cancers, uncontrolled infection, active enterocolitis, severe heart disease, severe drug allergy, cryoglobulinemia, or autoimmune disease, were excluded from the study. Those receiving systemic steroid therapy, who were pregnant or lactating, or who had brain metastasis and hypertension were also excluded. The research protocol was approved by the Ethical Committee of our institution and was registered at the University Hospital Medical Information Network Clinical Trials Registry (UMIN-CTR) (Unique trial number: UMIN000002136) on July 2, 2009. Written informed consent was obtained from each patient before they entered the study. The study was performed in accordance with the Declaration of Helsinki.

Generation of DCs

About 4 weeks after surgery, patients underwent leukapheresis to isolate peripheral blood mononuclear cells (PBMCs) using a Fresenius AS.TEC204 with the C4Y white blood cell set. Approximately 5 $\times 10^9$ PBMCs from each patient were allowed to adhere to tissue culture flasks in AIM-V medium (Invitrogen, Carlsbad, CA) at 37°C. After one hour, nonadherent cells were removed by washing with warm medium. To generate immature DCs, adherent PBMCs were cultured in AIM-V for 5 days in the presence of recombinant human granulocyte macrophage colony-stimulating factor (GM-CSF) (500 IU/ml; Berlex Laboratories, Montville, NJ) and recombinant human IL-4 (500 IU/ml; CellGenix Technologie Transfer GmbH, Freiburg, Germany). Immature DCs were then matured by adding GM-CSF (250 IU/ml), recombinant human IL-4 (250 IU/ml), tumor necrosis factor (TNF-α)

(0.01 μg/ml; CellGenix Technologie Transfer GmbH), prostaglandin E2 (PGE2) (1 μg/ml; Sigma, St. Louis, MO) and zoledronate (5 μM; Novartis, Basel, Switzerland) for a further 2 days [39].

Preparation of tumor lysates and electroloading of dendritic cells

Autologous tumor samples were obtained by surgery under aseptic conditions. Tumor tissues were minced with a scalpel in phosphate-buffered saline (PBS). The samples were then lysed by six freezing and thawing cycles, sonicated and centrifuged to produce tumor lysate. Finally the supernatant was filtered using 0.22-μm pore-size filters. The quantitation of total protein was performed using BCA Protein Assay Kit (Pierece Biotechnology, Rockford. IL, USA) according to the manufacturer's instruction. Colorimetric changes were detected by VersaMax microplate reader (Molecular Device Japan, Tokyo, JAPAN) at the wavelength of 562 nm with Softmax Pro software (Molecular Device Japan). Autologous tumor lysate was loaded into mature DCs using a MaxCyte GT electroporation-based system (MaxCyte Inc, Gaithersburg, MD) according to the manufacturer's instructions [40]. Tumor lysate-electroporated DCs, designated EP-DCs, were cryopreserved with 1 ml of autologous serum containing 10% DMSO and stored in liquid N_2 until use.

Immunization schedule

After leukapheresis, patients received sunitinib at a dose of 50 mg p.o. daily for 28 days followed by 14 days of rest. Two weeks after leukapheresis, patients received $1x10^7$ EP-DCs subcutaneously in the deltoid region; DC injection was repeated biweekly six times in total, extended to 12 for one long-surviving patient. For immunomonitoring, peripheral blood was drawn before DC therapy, at each treatment time point and 4 weeks after the last treatment. PBMCs were isolated by density gradient centrifugation using Lymphoprep (Axis-Shield, Oslo, Norway) and stored in liquid N_2 until use. Adverse events were graded according to National Cancer Institute-Common Terminology Criteria for Adverse Events version 4.0. Clinical responses were assessed by computed tomography and classified as complete response (CR), partial response (PR), stable disease (SD), or progressive disease (PD) according to the Response Evaluation Criteria in Solid Tumors (RECIST) criteria, version 1.1 [41].

IFN-γ secretion assay

PBMCs ($1x10^6$) from each time point and EP-DCs ($1x10^5$) were thawed and resuspended in AIM-V medium supplemented with 10% heat-inactivated pooled human serum (complete medium), and co-cultured in a 24-well plate at 37°C in a 5% CO_2 atmosphere for 2 days. Recombinant human IL-2 (Chiron, Emeryville, CA) was then added every 2–3 days to a final concentration of 50 IU/ml for another 12 days. The cultured PBMCs were harvested and used as responder cells, as described below. The IFN-γ secretion assay was carried out according to the manufacturer's protocol (Miltenyi Biotec, Bergisch Gladbach, Germany) [42]. Briefly, 1×10^6 responder cells were stimulated with 1×10^5 EP-DCs or mature DCs without electroporation (unloaded DCs) in complete medium for 4 hr at 37°C in a 5% CO_2 atmosphere. The cells were then washed and suspended in 100 μl of cold PBS, and treated with a mouse anti-IFN-γ antibody (IFN-γ catch reagent) (2 μl) for 5 min on ice. The cells were then diluted in complete medium (1 ml) and placed on a slowly rotating device (Miltenyi Biotec) to allow IFN-γ secretion at 37°C in a 5% CO_2 atmosphere. After incubation for 45 min, the cells were washed with cold PBS and treated with Fixable viability dye eFluor 450 (eBioscience, San Diego, CA), PE-labeled anti-IFN-γ (detection reagent), Alexa Fluor 647-labeled anti-human CD3 (Biolegend, San Diego, CA), PC5-labeled anti-human CD8 (Beckman Coulter, Fullerton, CA), and PECy7-labeled anti-human CD4 (Biolegend) mAbs. After incubation for 10 min at 4°C, the cells were washed and analyzed on a Gallios Flow Cytometer (Beckman Coulter).

Tregs and MDSCs

Analysis of Treg percentages in patient PBMC was carried out on thawed samples. Cells were stained in fluorescence-activated cell sorting (FACS) buffer (1× PBS with 2% heat-inactivated fetal bovine serum and 0.02% sodium azide). Nonspecific antibody binding was blocked by pretreatment with Clear Back (Human Fc receptor blocking reagent, MBL, Nagoya, Japan). Cells were stained with Dye450, Alexa Fluor 647-labeled anti-CD3, Alexa Fluor 488-labeled Foxp3, PE-Cy5-labeled CD4, and PE-labeled CD25 Abs according to the instructions for use of the Human Treg Flow Kit (Biolegend). MDSCs were also analyzed by FACS on thawed patient PBMC stained with Dye780, ECD-labeled CD14 (Beckman Coulter), FITC-labeled CD15 (Biolegend), PE-Cy5-labeled CD33 (Biolegend), and PE-labeled HLA-DR (BD Biosciences) Abs for 30 min at 4°C. Cells were washed in buffer and then fixed in 1% paraformaldehyde and analyzed by flow cytometry.

Delayed-type hypersensitivity (DTH)

EP-DCs or unloaded DCs were injected intradermally into different forearms. DTH reactions were evaluated 24 and 48 hours after the 6^{th} injection of DCs and considered to be positive when a skin reaction (>10 mm diameter of erythema) was triggered by EP-DCs but not unloaded DCs.

TH1/TH2 cytokine quantification

Amounts of IFN-γ, IL-1β, IL-2, IL-4, IL-5, IL-6, IL-8, IL-10, IL-12 p70, TNF-α, and TNF-β in patients' sera were quantified by a cytofluorometry-based ELISA system (Flowcytomix, Bender Medsystems GmbH, Austria). Standard curves for each cytokine were generated using the reference cytokine concentrations supplied by the manufacturer. Cytokines in sera from patients at different time points were estimated according to the manufacturer's instructions. Raw data of the FC bead assay were analyzed by FlowCytomixPro2.3 software.

Statistical analysis

The statistical analyses of immunological parameters and prognostic factors (PFS or OS) were performed using Wilcoxon signed-rank test and Kaplan-Meier method, respectively, with JMP software, version 9.0.3 (SAS Institute Inc., Cary, NC, USA).

Additional files

Additional file 1: The mean fluorescent intensity (MFI) of the surface expression of immunological molecules. Tabular data.

Additional file 2: Schedule for DC vaccination combined with sunitinib in this clinical trial. Supplementary figure.

Additional file 3: Data from an individual patient. Supplementary figure.

Additional file 4: Computed tomography (CT) images. Supplementary figure.

Abbreviations

RCC: Renal cell carcinoma; mRCC: Metastatic RCC; TKI: Tyrosine kinase inhibitor; MDSCs: Myeloid-derived suppressor cells; Tregs: Regulatory T cells; PBMCs: Peripheral blood mononuclear cells; GM-CSF: Granulocyte macrophage colony-stimulating factor; DCs: Dendritic cells; TNF-α: Tumor necrosis factor α; PGE2: Prostaglandin E2; OS: Overall survival; PFS: Progression-free survival; CR: Complete response; PR: Partial response; SD: Stable disease; PD: Progressive disease; RECIST: Response Evaluation Criteria in Solid Tumors; PBS: Phosphate-buffered saline.

Competing interests

Department of Immunotherapeutics is an endowed department supported by financial contributions from Medinet Co. Ltd. (Yokohama, Japan). Dr. Kazuhiro Kakimi received research support from Medinet Co. Ltd. The costs of the entire DC culture production and part of the immunological assays were covered by Medinet Co. Ltd. The study sponsors had no involvement in study design; collection, analysis, and interpretation of data; writing the report; and the decision to submit the report for publication. No potential conflicts of interest were disclosed by the other authors.

Authors' contributions

Conceived and designed the study: HM, YE, YH and KK. Performed the clinical study: HM, YE, HK, TN, HF, MS, TH, and KK. Analyzed the data: HM and KK. Wrote the paper: HM, YE, YH and KK. All authors read and approved the final manuscript.

Acknowledgements

We thank Makoto Kondo*, Takamichi Izumi*, and Takuya Takahashi* for performing DC cultures; Nao Fujieda*, Atsushi Kondo*, Kaori Kanbara* and Kohei Odaira* for immunological monitoring and laboratory assistance; Ryuji Maekawa*, Takashige Kondo*, Yoko Yamashita*, Tomoko Ishida*, Haruka Matsushita*, Yuki Nagasawa*, Hiroki Yoshihara* and Akiko Fukuzawa* for administrative supports. *MK, TI, TT, NF, AK, KK, KO, RM, TK, YY, TI, HM, YN, HY, and AF are employed by Medinet Co. Ltd. The part of this study (immunomonitoring) was performed as a research program of the Project for Development of Innovative research on Cancer Therapeutics (P-Direct), Ministry of Education, Culture, Sports, Science and Technology of Japan; this study was supported in part by a Grant-in-Aid for Scientific Research of the Ministry of Education, Culture, Sports, Science and Technology of Japan (Kazuhiro Kakimi, Yutaka Enomoto).

Author details

[1]Department of Immunotherapeutics, The University of Tokyo Hospital, 7-3-1 Hongo, Bunkyo-ku, Tokyo 113-8655, Japan. [2]Department of Urology, The University of Tokyo Hospital, 7-3-1 Hongo, Bunkyo-ku, Tokyo 113-8655, Japan. [3]Department of Urology, Mitsui Memorial Hospital, Izumicho 1, Kanda, Chiyoda-Ku, Tokyo 101-8643, Japan.

Received: 13 May 2014 Accepted: 30 July 2014
Published: 19 August 2014

References

1. Motzer RJ, Bander NH, Nanus DM: **Renal-cell carcinoma.** *N Engl J Med* 1996, 335:865–875.
2. Cohen HT, McGovern FJ: **Renal-cell carcinoma.** *N Engl J Med* 2005, 353:2477–2490.
3. Abe H, Kamai T: **Recent advances in the treatment of metastatic renal cell carcinoma.** *Int J Urol* 2013, 20:944–955.
4. Klapper JA, Downey SG, Smith FO, Yang JC, Hughes MS, Kammula US, Sherry RM, Royal RE, Steinberg SM, Rosenberg S: **High-dose interleukin-2 for the treatment of metastatic renal cell carcinoma.** *Cancer* 2008, 113:293–301.
5. Negrier S, Escudier B, Lasset C, Douillard J-Y, Savary J, Chevreau C, Ravaud A, Mercatello A, Peny J, Mousseau M, Philip T, Tursz T: **Recombinant human interleukin-2, recombinant human interferon alfa-2a, or both in metastatic renal-cell carcinoma.** *N Engl J Med* 1998, 338:1272–1278.
6. Fujioka T, Obara W, the Committee for Establishment of the Clinical Practice Guideline for the Management of Renal Cell C, the Japanese Urological A: **Evidence-based clinical practice guideline for renal cell carcinoma: the Japanese urological association 2011 update.** *Int J Urol* 2012, 19:496–503.
7. Flanigan RC, Mickisch G, Sylvester R, Tangen C, Van Poppel H, Crawford ED: **Cytoreductive nephrectomy in patients with metastatic renal cancer: a combined analysis.** *J Urol* 2004, 171:1071–1076.
8. Biswas S, Kelly J, Eisen T: **Cytoreductive nephrectomy in metastatic clear-cell renal cell carcinoma: perspectives in the tyrosine kinase inhibitor Era.** *Oncologist* 2009, 14:52–59.
9. May M, Brookman-May S, Hoschke B, Gilfrich C, Kendel F, Baxmann S, Wittke S, Kiessig S, Miller K, Johannsen M: **Ten-year survival analysis for renal carcinoma patients treated with an autologous tumour lysate vaccine in an adjuvant setting.** *Cancer Immunol Immunother* 2010, 59:687–695.
10. Azuma T, Horie S, Tomita K, Takahashi T, Tanaka Y, Kashiwase K, Nieda M, Takeuchi T, Ohta N, Shibata Y, Hirai H, Kitamura T: **Dendritic cell immunotherapy for patients with metastatic renal cell carcinoma: University of Tokyo experience.** *Int J Urol* 2002, 9:340–346.
11. Matsumoto A, Haraguchi K, Takahashi T, Azuma T, Kanda Y, Tomita K, Kurokawa M, Ogawa S, Takahashi K, Chiba S, Kitamura T: **Immunotherapy against metastatic renal cell carcinoma with mature dendritic cells.** *Int J Urol* 2007, 14:277–283.
12. Berntsen A, Trepiakas R, Wenandy L, Geertsen PF, thor Straten P, Andersen MH, Pedersen AE, Claesson MH, Lorentzen T, Johansen JS, Svane IM: **Therapeutic dendritic cell vaccination of patients with metastatic renal cell carcinoma: a clinical phase 1/2 trial.** *J Immunother* 2008, 31:771–780.
13. Gitlitz BJ, Belldegrun AS, Zisman A, Chao DH, Pantuck AJ, Hinkel A, Mulders P, Moldawer N, Tso C-L, Figlin RA: **A pilot trial of tumor lysate-loaded dendritic cells for the treatment of metastatic renal cell carcinoma.** *J Immunother* 2003, 26:412–419.
14. Höltl L, Zelle-Rieser C, Gander H, Papesh C, Ramoner R, Bartsch G, Rogatsch H, Barsoum AL, Coggin JH, Thurnher M: **Immunotherapy of metastatic renal cell carcinoma with tumor lysate-pulsed autologous dendritic cells.** *Clin Cancer Res* 2002, 8:3369–3376.
15. Soleimani A, Berntsen A, Svane IM, Pedersen AE: **Immune responses in patients with metastatic renal cell carcinoma treated with dendritic cells pulsed with tumor lysate.** *Scand J Immunol* 2009, 70:481–489.
16. Rabinovich GA, Gabrilovich D, Sotomayor EM: **Immunosuppressive strategies that are mediated by tumor cells.** *Annu Rev Immunol* 2007, 25:267–296.

17. Pardoll DM: **The blockade of immune checkpoints in cancer immunotherapy.** *Nat Rev Cancer* 2012, **12**:252–264.
18. Yang JC, Hughes M, Kammula U, Royal R, Sherry RM, Topalian SL, Suri KB, Levy C, Allen T, Mavroukakis S, Lowy I, White DE, Rosenberg SA: **Ipilimumab (anti-CTLA4 antibody) causes regression of metastatic renal cell cancer associated with enteritis and hypophysitis.** *J Immunother* 2007, **30**:825–830.
19. Lipson EJ, Sharfman WH, Drake CG, Wollner I, Taube JM, Anders RA, Xu H, Yao S, Pons A, Chen L, Pardoll DM, Brahmer JR, Topalian SL: **Durable cancer regression Off-treatment and effective reinduction therapy with an anti-PD-1 antibody.** *Clin Cancer Res* 2013, **19**:462–468.
20. Topalian SL, Hodi FS, Brahmer JR, Gettinger SN, Smith DC, McDermott DF, Powderly JD, Carvajal RD, Sosman JA, Atkins MB, Leming PD, Spigel DR, Antonia SJ, Horn L, Drake CG, Pardoll DM, Chen L, Sharfman WH, Anders RA, Taube JM, McMiller TL, Xu H, Korman AJ, Jure-Kunkel M, Agrawal S, McDonald D, Kollia GD, Gupta A, Wigginton JM, Sznol M: **Safety, activity, and immune correlates of anti–PD-1 antibody in cancer.** *N Engl J Med* 2012, **366**:2443–2454.
21. Brahmer JR, Tykodi SS, Chow LQM, Hwu W-J, Topalian SL, Hwu P, Drake CG, Camacho LH, Kauh J, Odunsi K, Pitot HC, Hamid O, Bhatia S, Martins R, Eaton K, Chen S, Salay TM, Alaparthy S, Grosso JF, Korman AJ, Parker SM, Agrawal S, Goldberg SM, Pardoll DM, Gupta A, Wigginton JM: **Safety and activity of anti–PD-L1 antibody in patients with advanced cancer.** *N Engl J Med* 2012, **366**:2455–2465.
22. Zea AH, Rodriguez PC, Atkins MB, Hernandez C, Signoretti S, Zabaleta J, McDermott D, Quiceno D, Youmans A, O'Neill A, Mier J, Ochoa AC: **Arginase-producing myeloid suppressor cells in renal cell carcinoma patients: a mechanism of tumor evasion.** *Cancer Res* 2005, **65**:3044–3048.
23. Mirza N, Fishman M, Fricke I, Dunn M, Neuger AM, Frost TJ, Lush RM, Antonia S, Gabrilovich DI: **All-trans-retinoic acid improves differentiation of myeloid cells and immune response in cancer patients.** *Cancer Res* 2006, **66**:9299–9307.
24. Hiles JJ, Kolesar JM: **Role of sunitinib and sorafenib in the treatment of metastatic renal cell carcinoma.** *Am J Health Syst Pharm* 2008, **65**:123–131.
25. Motzer RJ, Hutson TE, Tomczak P, Michaelson MD, Bukowski RM, Rixe O, Oudard S, Negrier S, Szczylik C, Kim ST, Chen I, Bycott PW, Baum CM, Figlin RA: **Sunitinib versus interferon Alfa in metastatic renal-cell carcinoma.** *N Engl J Med* 2007, **356**:115–124.
26. Escudier B, Eisen T, Stadler WM, Szczylik C, Oudard S, Siebels M, Negrier S, Chevreau C, Solska E, Desai AA, Rolland F, Demkow T, Hutson TE, Gore M, Freeman S, Schwartz B, Shan M, Simantov R, Bukowski RM: **Sorafenib in advanced clear-cell renal-cell carcinoma.** *N Engl J Med* 2007, **356**:125–134.
27. Ko JS, Zea AH, Rini BI, Ireland JL, Elson P, Cohen P, Golshayan A, Rayman PA, Wood L, Garcia J, Dreicer R, Bukowski R, Finke JH: **Sunitinib mediates reversal of myeloid-derived suppressor cell accumulation in renal cell carcinoma patients.** *Clin Cancer Res* 2009, **15**:2148–2157.
28. Ozao-Choy J, Ma G, Kao J, Wang GX, Meseck M, Sung M, Schwartz M, Divino CM, Pan P-Y, Chen S-H: **The novel role of tyrosine kinase inhibitor in the reversal of immune suppression and modulation of tumor microenvironment for immune-based cancer therapies.** *Cancer Res* 2009, **69**:2514–2522.
29. Finke JH, Rini B, Ireland J, Rayman P, Richmond A, Golshayan A, Wood L, Elson P, Garcia J, Dreicer R, Bukowski R: **Sunitinib reverses type-1 immune suppression and decreases T-regulatory cells in renal cell carcinoma patients.** *Clin Cancer Res* 2008, **14**:6674–6682.
30. Hipp MM, Hilf N, Walter S, Werth D, Brauer KM, Radsak MP, Weinschenk T, Singh-Jasuja H, Brossart P: **Sorafenib, but not sunitinib, affects function of dendritic cells and induction of primary immune responses.** *Blood* 2008, **111**:5610–5620.
31. Xin H, Zhang C, Herrmann A, Du Y, Figlin R, Yu H: **Sunitinib inhibition of Stat3 induces renal cell carcinoma tumor cell apoptosis and reduces immunosuppressive cells.** *Cancer Res* 2009, **69**:2506–2513.
32. Kujawski M, Kortylewski M, Lee H, Herrmann A, Kay H, Yu H: **Stat3 mediates myeloid cell–dependent tumor angiogenesis in mice.** *J Clin Invest* 2008, **118**:3367–3377.
33. Ko JS, Rayman P, Ireland J, Swaidani S, Li G, Bunting KD, Rini B, Finke JH, Cohen PA: **Direct and differential suppression of myeloid-derived suppressor cell subsets by Sunitinib is compartmentally constrained.** *Cancer Res* 2010, **70**:3526–3536.
34. Waugh DJJ, Wilson C: **The interleukin-8 pathway in cancer.** *Clin Cancer Res* 2008, **14**:6735–6741.
35. Huang D, Ding Y, Zhou M, Rini BI, Petillo D, Qian C-N, Kahnoski R, Futreal PA, Furge KA, Teh BT: **Interleukin-8 mediates resistance to antiangiogenic agent Sunitinib in renal cell carcinoma.** *Cancer Res* 2010, **70**:1063–1071.
36. Eikawa S, Ohue Y, Kitaoka K, Aji T, Uenaka A, Oka M, Nakayama E: **Enrichment of Foxp3+ CD4 regulatory T cells in migrated T cells to IL-6– and IL-8–expressing tumors through predominant induction of CXCR1 by IL-6.** *J Immunol* 2010, **185**:6734–6740.
37. Chen DS, Mellman I: **Oncology meets immunology: the cancer-immunity cycle.** *Immunity* 2013, **39**:1–10.
38. Vanneman M, Dranoff G: **Combining immunotherapy and targeted therapies in cancer treatment.** *Nat Rev Cancer* 2012, **12**:237–251.
39. Takahara M, Miyai M, Tomiyama M, Mutou M, Nicol AJ, Nieda M: **Copulsing tumor antigen-pulsed dendritic cells with zoledronate efficiently enhance the expansion of tumor antigen-specific CD8+ T cells via Vγ9γδ T cell activation.** *J Leukoc Biol* 2008, **83**:742–754.
40. Weiss JM, Allen C, Shivakumar R, Feller S, Li L-H, Liu LN: **Efficient responses in a murine renal tumor model by electroloading dendritic cells with whole-tumor lysate.** *J Immunother* 2005, **28**:542–550.
41. Eisenhauer EA, Therasse P, Bogaerts J, Schwartz LH, Sargent D, Ford R, Dancey J, Arbuck S, Gwyther S, Mooney M, Rubinstein L, Shankar L, Dodd L, Kaplan R, Lacombe D, Verweij J: **New response evaluation criteria in solid tumours: revised RECIST guideline (version 1.1).** *Eur J Cancer* 2009, **45**:228–247.
42. Desombere I, Meuleman P, Rigole H, Willems A, Irsch J, Leroux-Roels G: **The interferon gamma secretion assay: a reliable tool to study interferon gamma production at the single cell level.** *J Immunol Methods* 2004, **286**:167–185.

doi:10.1186/s40425-014-0030-4
Cite this article as: Matsushita *et al.*: A pilot study of autologous tumor lysate-loaded dendritic cell vaccination combined with sunitinib for metastatic renal cell carcinoma. *Journal for ImmunoTherapy of Cancer* 2014 2:30.

OPEN ACCESS Freely available online

PLOS ONE

Denatured Mammalian Protein Mixtures Exhibit Unusually High Solubility in Nucleic Acid-Free Pure Water

Junichiro Futami[1]*, Haruna Fujiyama[1], Rie Kinoshita[1], Hidenori Nonomura[1], Tomoko Honjo[1], Hiroko Tada[1], Hirokazu Matsushita[2], Yoshito Abe[3], Kazuhiro Kakimi[2]

1 Department of Biotechnology, Graduate School of Natural Science and Technology, Okayama University, Okayama, Japan, **2** Department of Immunotherapeutics, The University of Tokyo Hospital, Tokyo, Japan, **3** Department of Protein Structure, Function and Design, Graduate School of Pharmaceutical Sciences, Kyushu University, Fukuoka, Japan

Abstract

Preventing protein aggregation is a major goal of biotechnology. Since protein aggregates are mainly comprised of unfolded proteins, protecting against denaturation is likely to assist solubility in an aqueous medium. Contrary to this concept, we found denatured total cellular protein mixture from mammalian cell kept high solubility in pure water when the mixture was nucleic acids free. The lysates were prepared from total cellular protein pellet extracted by using guanidinium thiocyanate-phenol-chloroform mixture of TRIzol, denatured and reduced total protein mixtures remained soluble after extensive dialysis against pure water. The total cell protein lysates contained fully disordered proteins that readily formed large aggregates upon contact with nucleic acids or salts. These findings suggested that the highly flexible mixtures of disordered proteins, which have fully ionized side chains, are protected against aggregation. Interestingly, this unusual solubility is characteristic of protein mixtures from higher eukaryotes, whereas most prokaryotic protein mixtures were aggregated under identical conditions. This unusual solubility of unfolded protein mixtures could have implications for the study of intrinsically disordered proteins in a variety of cells.

Citation: Futami J, Fujiyama H, Kinoshita R, Nonomura H, Honjo T, et al. (2014) Denatured Mammalian Protein Mixtures Exhibit Unusually High Solubility in Nucleic Acid-Free Pure Water. PLoS ONE 9(11): e113295. doi:10.1371/journal.pone.0113295

Editor: Reza Khodarahmi, Kermanshah University of Medical Sciences, Islamic Republic of Iran

Received August 21, 2014; **Accepted** October 22, 2014; **Published** November 18, 2014

Data Availability: The authors confirm that all data underlying the findings are fully available without restriction. All relevant data are within the paper.

Funding: This work was supported by the grants from the Japan Society for the Promotion of Science (JSPS: http://www.jsps.go.jp/english/index.html) for Junichiro Futami (JSPS KAKENHI Grant Numbers 23360370 and 24656506). The funders had no role in study design, data collection and analysis, decision to publish, or preparation of the manuscript.

Competing Interests: The authors have declared that no competing interests exist.

* Email: futamij@okayama-u.ac.jp

Introduction

Proteins perform an extraordinary array of functions in cells [1]. To understand the behavior of proteins in living cells, we must consider the extremely high intracellular concentrations of macromolecules. The cytoplasmic protein concentration has been estimated to be 100 mg/mL [2], and the total macromolecular concentration (including proteins, lipids, nucleic acids, and sugars) could be as high as 400 mg/mL [3]. Proteins have therefore evolved to exert their biological functions under highly crowded conditions, which raises the question of how they maintain solubility in such a dense milieu. Intrinsically unstructured proteins display unusually high solubility, and studying these molecules may elucidate the mechanisms underlying this phenomenon.

Proteins must fold into unique three-dimensional structures and interact specifically with particular molecules to function correctly. However, some proteins exist in an intrinsically unstructured form, lacking stable secondary and tertiary structural elements, but retaining full functionality. These intrinsically disordered proteins (IDPs) are unfolded *in vitro*, but may adopt functional conformations *in vivo*, although several lines of indirect evidence indicate that IDPs remain disordered in the cell [4,5]. The capacity for folding or remaining intrinsically unstructured mainly depends on the interplay between water molecules and the characteristic amino acid composition that dictate the hydrophobicity, charge, and flexibility [6,7]. Generally, IDPs lack bulky hydrophobic residues such as Ile, Leu, and Val, as well as aromatic residues such as Trp, Tyr, and Phe but are enriched in polar residues such as Arg, Gly, Gln, Ser, Pro, Glu and Lys, and the secondary structure-breaking amino acids Gly and Pro [6,7]. This composition results in high solubility in water despite being highly unstructured. Much work has been done on prediction of IDPs from protein sequences, and this class of proteins are much more abundant in eukaryotes than in prokaryotes [8,9]. Although the predicted disorder depends on the program used, intrinsically disordered regions (IDRs) account for 8–10% of protein sequences in prokaryotes and 30–41% in eukaryotes [10,11]. The majority of cellular proteins are predicted to adopt fully folded biologically active conformations, but IDRs are abundant. Unlike globular proteins, IDPs show unusually high solubility following heat treatment. Kim *et al* (2000) demonstrated that 20% of total proteins in Jurkat T-cell lysates are heat-resistant and remain soluble after boiling [12]. The resultant soluble protein fractions

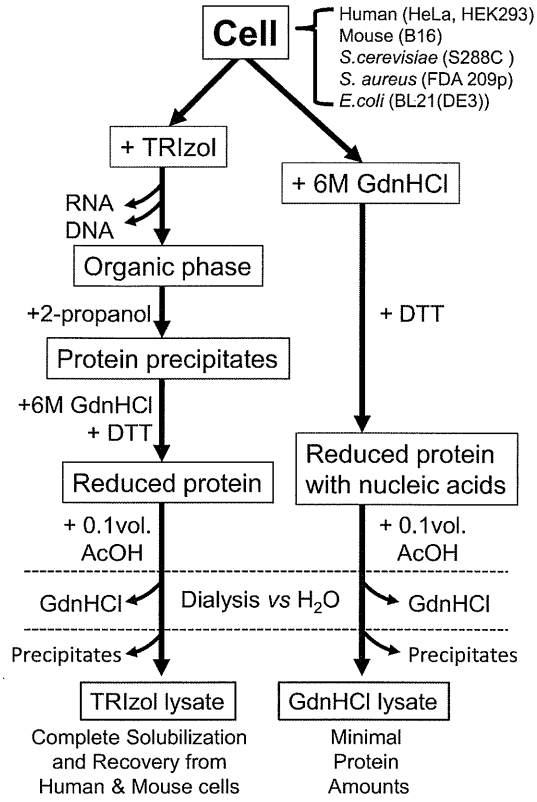

Figure 1. Schematic representation of the preparation of total cell protein lysates.
doi:10.1371/journal.pone.0113295.g001

are enriched in IDPs and are a valuable resource for proteomic research [13,14].

It is widely accepted that denaturing proteins exposes hydrophobic residues that are normally buried in the native conformation, and aggregation is mainly mediated by the resulting hydrophobic or electrostatic interactions between individual molecules. Hydrophobic interactions mainly occur between neighboring denatured protein molecules, whereas electrostatic interactions mainly occur between denatured proteins and anionic nucleic acid polymers. Removal of nucleic acids is therefore critical for efficient oxidative refolding of globular proteins from bacterial inclusion bodies [15]. The refolding efficiency can be improved by altering the ionic strength, pH, and using additives [16], but the final yield of refolded protein is often decreased substantially due to the presence of misfolded protein molecules that seed aggregation during purification steps. Poor protein solubility is a commonly encountered problem, and maintaining proteins in soluble conditions is the conventional approach for ensuring biological activity is maintained. The opposite approach of intentional denaturation is unusual, but may work well for maintaining the solubility of IDPs.

The unusual high solubility of mammalian IDPs appeared to be characteristic of proteins from higher eukaryotes, since most prokaryotic protein mixtures aggregated under similar denaturing conditions. Although the detailed mechanism is unclear, this unusual solubility presumably reflects the amino acid composition of eukaryotic IDPs, and likely reflects key evolutionary differences.

Materials and Methods

Cell culture

Human cell lines HeLa S3 and HEK293 PEAKrapid, and the mouse cell line B16 melanoma-F10 were purchased from ATCC. All cell lines were cultured in Dulbecco's modified Eagle's medium (DMEM) supplemented with 10% fetal bovine serum (FBS, PAA laboratories, Austria) and penicillin/streptomycin (Wako, Osaka, Japan). *S. cerevisiae*, S288C (National Bio-Resource Project of the MEXT, Japan) was grown in YPD media at 30°C for 24 h. *S. aureus* (FDA 209P) in brain Bacto heart infusion medium (BD Biosciences), and *E. coli* BL21 (DE3) (Novagen) in LB medium were grown at 37°C for 24 h. *E. coli* BL21 (DE3) containing pET23a-human β-actin plasmid DNA were used to express human β-actin. Transformed cells were cultured in LB at 37°C, expression was induced with 0.4 mM IPTG, and growth continued for 3 h.

Isolation of nucleic acid-free total cell proteins

Total cell proteins were isolated using TRIzol (Invitrogen) according to the manufacturer's instructions. Briefly, sub-confluent mammalian cells cultured on a 100 mm dish were washed twice with PBS, lysed in 5 mL TRIzol, scraped off and transferred to a centrifuge tube. Proteins were recovered in the organic phase following addition of chloroform, and precipitated by addition of 2-propanol. Protein precipitates were extensively washed with 0.3 M GdnHCl in 95% ethanol at least five times, to give a white protein pellet that was washed three times with ethanol. Ethanol-wet pellets were used directly as they were poorly soluble in 6 M GdnHCl after drying. Cell pellets of *S. cerevisiae*, *S. aureus*, *and E. coli* (0.2 g wet weight were dissolved in 1 mL TRIzol and treated as described above.

Preparation of protein lysates in salt-free water

Total cell proteins were dissolved in 6 M GdnHCl containing 0.1 M Tris-HCl pH 8.5, and the protein concentration was adjusted for each experiment using values determined from the absorbance at 280 nm, assuming 1 absorbance unit at 280 = 1 mg/mL. Disulfide bonds were then reduced with 0.1 M DTT at 37°C for 1 h, and a 0.1 volume of acetic acid was added. The resultant protein solutions were dialyzed extensively against Milli-Q water using a Slide-A-Lyzer (3.5K MWCO, Thermo Fisher Scientific, Waltham, MA) at 4°C for 48 h. The Milli-Q water was changed every few hours initially then every 12–16 h. Residual nucleic acids in TRIzol lysate were determined with Quant-iT PicoGreen dsDNA and RiboGreen RNA Assay Kit (Life Technologies, Carlsbad, CA). To determine the solubility in TRIzol lysates, initial protein concentrations were adjusted to 1 mg/mL before starting dialysis. Aggregated proteins and the remaining soluble proteins were separated by centrifugation at 14,000×*g* for 15 min at 4°C, and each was solubilized in 8 M urea prior to protein concentration measurement using the Bradford protein assay (Bio-Rad Laboratories, Hercules, CA) with bovine serum albumin as a standard.

Determination of protein solubility in lysates containing additives

Nucleic acid-free total cell protein lysates (TRIzol lysates) from HeLa cells in Milli-Q water and with a protein concentration of 2–3 mg/mL and a pH of 5 and an electrical conductivity <20 μS/cm were used for assays. dNTPs (Thermo) 16S-rRNA and 23S-rRNA from *E. coli* MRE600 (Boehringer Mannheim, Germany), tRNA from baker's yeast (Type X-SA, Sigma, St. Louis, MO), or DNA from calf thymus (phenol-chloroform extracted, <2000 bp,

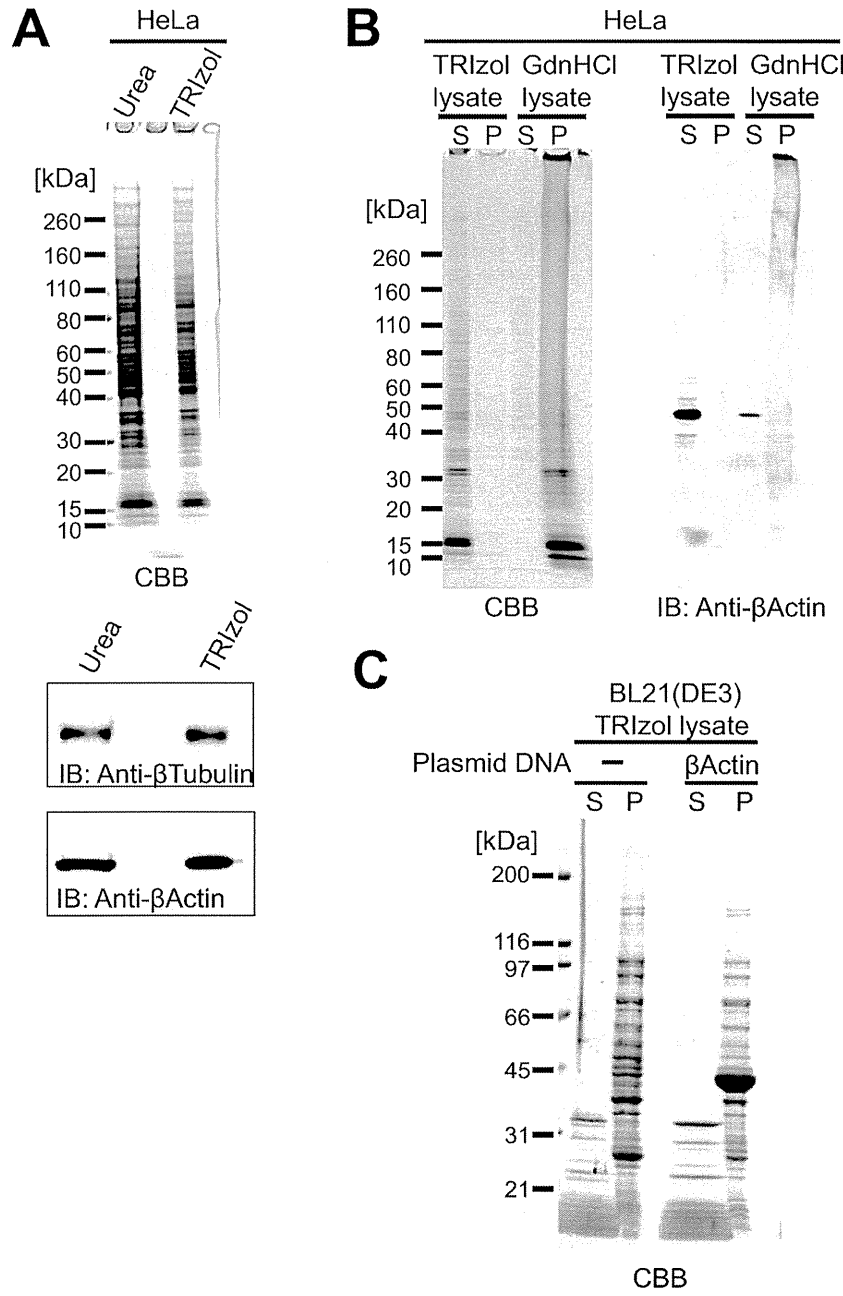

Figure 2. Analysis of total cell protein lysates. A. SDS-PAGE of total cell proteins lysed with 8 M urea or precipitated from the organic phase of TRIzol homogenates (an equivalent number of HeLa cells were used in each case). Endogenous proteins were also analyzed using western blotting. **B.** SDS-PAGE of total cell protein TRIzol and GdnHCl lysates. Equivalent amounts of protein in soluble fractions (S) and precipitates (P) following centrifugation were loaded. **C.** SDS-PAGE of TRIzol lysates prepared from *E. coli* BL21(DE3) expressing or not expressing human β-actin.
doi:10.1371/journal.pone.0113295.g002

WAKO) were mixed with TRIzol lysates to give a protein concentration of 0.1 mg/mL, and incubated for 60 min at 4°C. After centrifugation at 14,000×*g* for 15 min at 4°C, the concentration of soluble proteins was determined by Bradford protein assay (Bio-Rad).

Plasmid transfection and functional assays

Plasmids for expression of the enhanced GFP (pEGFP-N1; Clontech, Mountainview, CA) and firefly luciferase (Luc; pGL3-basic; Promega, Madison, WI) were used to transfect HEK293 PEAKrapid cells using 293 fectin (Invitrogen) which were subsequently cultured for 24 h. To prepare native protein lysates, cells were lysed with Glo Reporter Lysis Buffer (GLB, Promega). The fluorescence intensity of EGFP-containing lysates was analyzed using a Multi Microplate Reader MTP-800 (Hitachi, Japan) at Ex/Em: 480/530 nm. Luminescence of Luc-containing lysates was measured using a steady Glo assay kit (Promega) and Luminometer Junior LB9509 (Berthold Technologies, Dak Ridge, TN).

Table 1. Solubility of denatured and nucleic acid-free total cell proteins in pure water.

Source	Solubility in TRIzol lysate (%)*
H. Sapien, M. musculus (HeLa, Hek293, B16–F10)	95.9±1.7
S.cerevisiae (S288C)	59.1±8.4
S. aureus (FDA209p)	47.3±0.9
E.coli (BL21(DE3))	32.9±3.0

*Initial protein concentrations were adjusted to 1 mg/mL before dialysis.
doi:10.1371/journal.pone.0113295.t001

Western blotting

Endogenous and transiently expressed reporter protein levels were verified by Western blotting using conventional procedures using the following primary antibodies; anti-β-actin (13E5, Cell Signaling Technologies, Beverly, MA), β-tubulin (Cell Signaling Technologies), GFP (mFX75, Wako), Luciferase (MBL, Nagoya, Japan). Membranes were treated with horseradish peroxidase-conjugated anti-mouse IgG or anti-rabbit IgG (Cell Signaling Technology), and positive signals were measured using a chemiluminescence system.

NMR

NMR spectra were recorded at 37°C on a Varian Unity INOVA 600 spectrometer (Varian, CA). 3Hmutwil and *S*-carboxymethylated mouse lysozyme were prepared as described previously [17–19], and 0.1 mM samples of ^{15}N-labeled proteins were dissolved in TRIzol lysates or distilled water containing 10% D_2O. The pH was adjusted to 2 using HCl, and NH signal assignments from ^{1}H-^{15}N-labeled HSQC spectra were assigned as described [19].

Results

Preparation of nucleic acid-free total cell protein lysates

In order to prepare nucleic acid-free total protein lysates from cultured mammalian cells under native conditions, we removed nucleic acids using three different approaches; selective precipitation with polyethylenimine [20], extensive digestion with nuclease, and chromatographically using an anion-exchange column. Unfortunately, neither method produced a satisfactory yield or purity. In contrast, phenol-chloroform extraction was efficient at ensuring total separation of nucleic acids and denatured total cell proteins. The guanidinium thiocyanate-phenol-chloroform mixture that constitutes TRIzol reagent, that is regularly used for RNA preparation [21], was used to homogenize cells, and proteins extracted using this reagent have been successfully recovered for proteomic research [22–24]. In this extraction procedure, proteins are fractionated into the organic phase and precipitated by addition of 2-propanol (Fig. 1), and 90% of total cellular proteins can be recovered, which is considerably higher than was achieved by homogenizing cells directly in 8 M Urea (Fig. 2A). After extensive washes with 0.3 M guanidine hydrochloride (GdnHCl)-95% ethanol, or in ethanol, total cellular proteins were recovered as a tightly packed white pellet following centrifugation, which was used directly or stored at −20°C as a wet pellet to avoid the difficulties associated with resuspending dried pellets in denaturant solutions. When dissolved in 6 M GdnHCl, proteins formed a slightly cloudy solution that clarified following reduction with dithiothreitol (DTT). Proteins were successfully solubilized following dialysis against pure water at acidic pH (Fig. 2 and Table 1) to give a yield of approximately 6 mg/mL from HeLa cells. The pH of the TRIzol lysate was between 5 and 5.8, which was the same as the dialysis solution, confirming dialysis had gone to completion. The electrical conductivity of the TRIzol lysate was less than 20 μS/cm, which was estimated to be less than 1 mM of electrolytes and is probably mostly residual GdnHCl. All Trizol lysates confirmed to show UV absorption spectrum has a peak maximum at approximately 280 nm. The residual nucleic acids in HeLa TRIzol lysate were less than 1 ng/mL in 1 mg/mL of protein by fluorescent nucleic acids detection methods, thus the lysates were virtually nucleic acids free. As shown in Figure 2A, denatured mammalian proteins in nucleic acid-free water showed unexpectedly high solubility compared with the extensive insoluble aggregation observed in denaturant containing nucleic acids (Fig. 1, 2B). Total cellular proteins from another eukaryote (*Saccharomyces cerevisiae*) and two prokaryotes (*Staphylococcus*

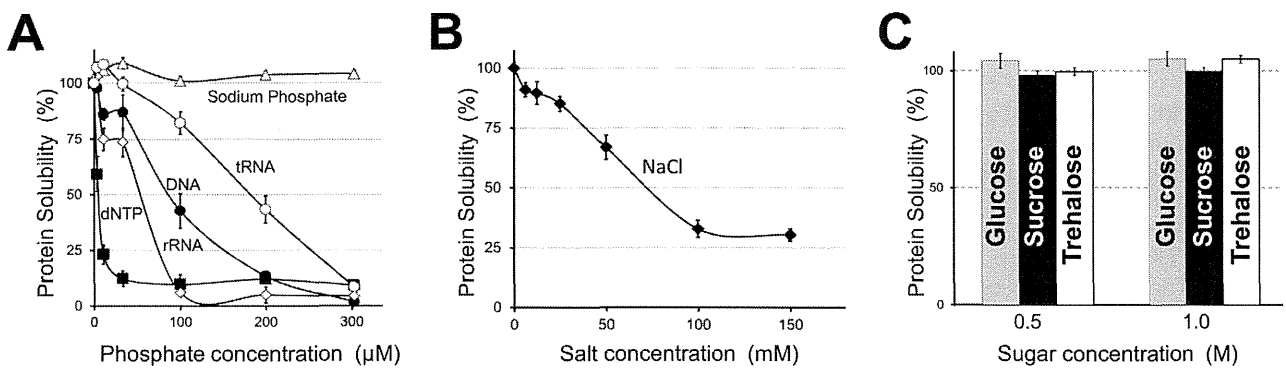

Figure 3. Effect of additives on protein solubility in HeLa cell TRIzol lysates. The solubility of proteins remaining after addition of nucleic acids (**A**), sodium chloride (**B**) or carbohydrates (**C**) was determined.
doi:10.1371/journal.pone.0113295.g003

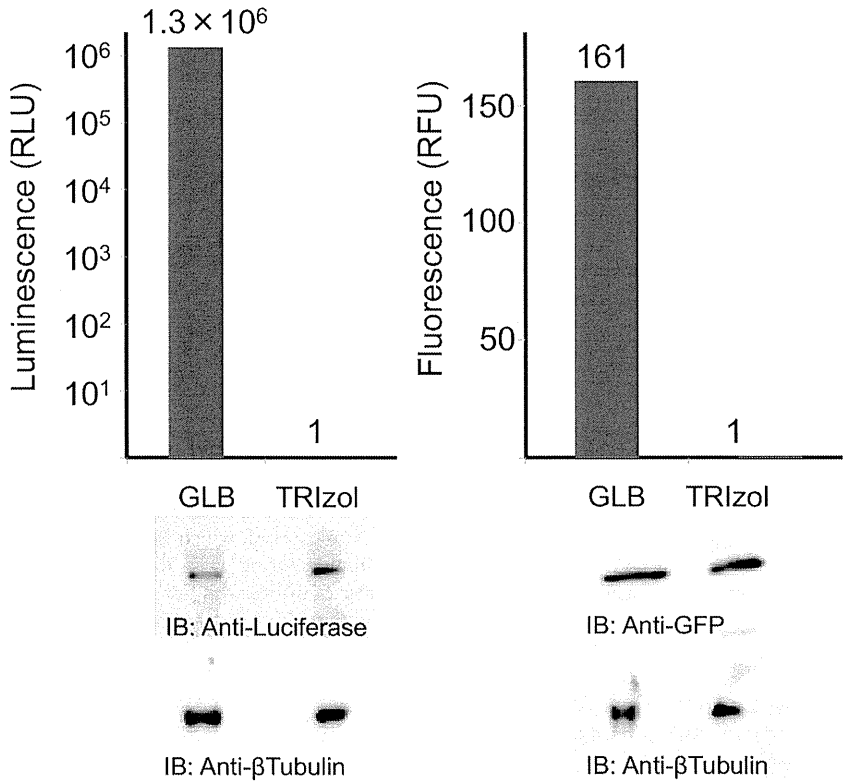

Figure 4. Biological activity of reporter proteins in physiological buffer or TRIzol lysates. Hek293 cells expressing either GFP or Luc were directly lysed in physiological Glo Lysis buffer (GLB) or TRIzol, and GFP or Luc activity were measured. Reporter proteins were verified by western blotting.
doi:10.1371/journal.pone.0113295.g004

aureus and *Escherichia coli*) showed reduced solubility (Table 1). However, low molecular weight (<20 kDa) denatured proteins from *E. coli* were soluble in these conditions, whereas most higher molecular weight (>30 kDa) proteins were insoluble (Figure 2C). Recombinant human β -actin is expressed in inclusion bodies in *E. coli*, and is known to be highly insoluble in the denatured form [25]. This protein remained insoluble in the *E. coli* total protein lysate even in nucleic acid-free conditions (Fig. 2C). In contrast, denatured β-actin from HeLa cells showed high solubility in nucleic acid-free conditions (Fig. 2B). The high solubility and resistance to aggregation of mammalian total cellular proteins in nucleic acid-free pure water compared to prokaryotic proteins (Table 1) presumably reflects an evolutionary divergence, which is consistent with the high abundance of IDPs in eukaryotes but not in prokaryotes.

Effect of additives on the solubility of TRIzol-solubilized proteins from HeLa cells

Nucleic acids at a concentration of 100−300 μM of phosphate group (30–100 μg/mL) induced precipitation of TRIzol-solubilized proteins from HeLa cells. Interestingly, the triphosphate group of dNTPs appeared to be a strong inducer of precipitation of denatured proteins, whereas monophosphate anions showed no such effect in the concentration range studied (Fig. 3A). The ionic strength was also important for solubility; the solubility of proteins in physiological saline decreased to 30% (Fig. 3B). However, non-ionic solutes such as sugars did not affect protein solubility (Fig. 3C), indicating that coulomb interactions between denatured proteins and additives contributed to protein solubility in TRIzol lysates. Although the pH can be an important factor affecting the net charge of protein molecules, this proved difficult to determine to analyze here, because addition of ionic buffers rapidly induced protein aggregation at all pH values tested.

Protein conformation in TRIzol lysates

To confirm that proteins were completely denatured in TRIzol lysates, HEK293 cells expressing Luciferase or GFP were examined. As shown in Figure 4, both cell types were successfully lysed in Glo Reporter Lysis Buffer (GLB, Promega) under native conditions in which the reporter protein function was maintained. While ensuring the same number of each cell type was used, reporter proteins were successfully recovered in soluble but denatured (non-functional) form in TRIzol lysates. In a previous study, immunoglobulin light chain derived amyloidogenic 3Hmut at pH 2 [19] and *S*-carboxylmethylated mouse lysozyme at pH 5 [17] were confirmed to be fully disordered using heteronuclear NMR spectroscopy [18,26]. Using these disordered proteins as probes, ^{1}H-^{15}N heteronuclear single quantum coherence (HSQC) spectra were compared for HeLa TRIzol lysates. As shown in Figure 5, the overall spectra for both proteins exhibited similar crowded resonances indicative of fully denatured proteins. These results confirmed that the proteins in the HeLa cell lysates were fully unfolded and highly soluble.

Discussion

In this study, we observed that fully denatured mammalian total cell protein mixtures showed unusually high solubility in nucleic acid-free pure water. This unusual solubility appeared to be

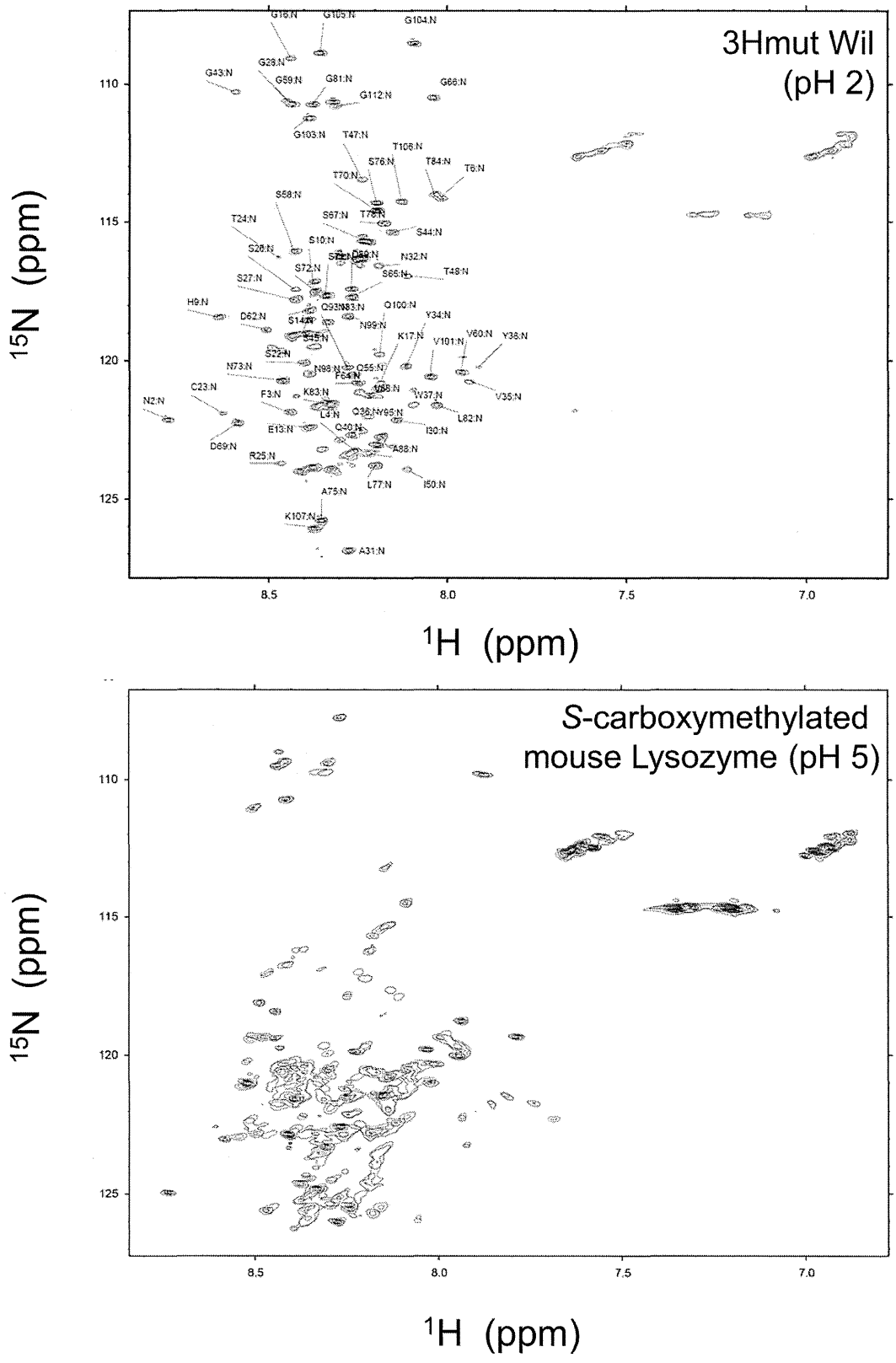

Figure 5. Effect of water soluble denatured protein mixtures on the solution structure of intrinsically disordered proteins. ^{1}H-^{15}N HSQC spectra of the intrinsically disordered 3HmutWil and *S*-carboxymethylated mouse lysozyme in the absence (black) and presence (red) of HeLa cell TRIzol lysates. Assignments of 3HmutWil in the absence of lysate are indicated.
doi:10.1371/journal.pone.0113295.g005

characteristic of higher eukaryotes, since proteins from a lower eukaryote (yeast) and two prokaryotes were largely aggregated under comparable conditions. This observation likely reflects a key evolutionary divide since IUPs are known to be highly abundant in mammalian cells [10,11]. Within the single-celled organisms studied, denatured proteins from the eukaryote *Saccharomyces cerevisiae* showed higher solubility than did those from two prokaryotes (Table 1). This trend was consistent with previous studies on IDPs from *Saccharomyces cerevisiae* and *E. coli* [27]. Therefore, in a salt-free and nucleic acid-free environment, the solubility of denatured proteins is highly correlated with the flexibility of the polypeptide and the proportion of hydrophilic residues in the protein chain.

Reconstitution of nucleic acids into TRIzol lysates from the HeLa cells indicated that these polyanionic macromolecules strongly promote the aggregation of denatured proteins. As shown in Figure 3A, tRNA, which is a tightly folded molecule, induced protein aggregation to a lesser degree than did dNTPs that have exposed phosphate groups. Thus, the electrostatic interactions between nucleic acids and denatured protein molecules could be a strong trigger for protein aggregation. This may explain why mammalian recombinant proteins frequently aggregate in bacterial cells. In our previous study, recombinant proteins isolated from bacterial inclusion bodies were found to be tightly associated with nucleic acid [15].

The ionic strength of TRIzol lysates also affected protein solubility significantly (Fig. 3B). Unfolded purified proteins, including integral membrane proteins, have been successfully solubilized in pure water previously [6,7,28–30]. Furthermore, the structural and dynamic properties of proteins in 8 M urea and pure water were shown to be similar using NMR [31]. Soluble proteins in pure water are predicted to be highly flexible due to strong intramolecular and intermolecular electrostatic repulsion [30]. In this study, pure water had a pH of 5.6, presumably due to the atmospheric carbon dioxide concentration. At this pH, ionizable groups on Lys, Arg, His, Asp, and Glu residues are potentially fully charged in the absence of counter ions, which maximizes the hydration of unfolded proteins. The high entropy of the denatured proteins in the HeLa cell TRIzol lysates is presumably the reason for the high solubility. Since aggregation requires productive collisions between protein molecules, enthalpy-entropy compensation theory can explain the unusually high solubility of denatured mammalian proteins in pure water [32,33].

Although the detailed mechanism is unclear, flexible polypeptide chains classified as IDPs may competitively suppress intermolecular interactions between otherwise insoluble hydrophobic polypeptides. Mammalian proteins in TRIzol lysates retained solubility for more than 6 months at 4°C. Importantly, approximately 30% of fully disordered proteins in mixtures from human cells maintained solubility in physiological saline (Fig. 3B). Competitive suppression of protein aggregation may partially explain the extraordinarily high solubility of mammalian proteins in living cells.

Upon screening of aggregation-prone protein domains, highly charged intrinsically disordered flexible sequences termed entropic bristles served as effective solubilizers in fusion partner proteins [33–35]. This suggests that disordered regions in IDPs enhance protein solubility via entropic effects, and pure water may enhance this effect. Chemical protein cationization of Cys residues is a powerful approach for solubilization of denatured proteins [17,36,37], which also enhances protein flexibility via electrostatic effects. Enhancing protein flexibility therefore appears to be a productive strategy for increasing the solubility of disordered proteins.

Solubilization of proteins is essential for their use in biotechnological and medical applications. Maintaining the biologically active 'native' conformation is the preferred approach for soluble proteins. In the case of denatured proteins, especially those of mammalian origin, nucleic acid-free pure water may be a useful solvent for the alternative approach of solubilizing disordered proteins. This alternative approach could be applied in numerous ways. For example, surgically removed cancer tissues contain immunologically important antigens that induce cancer immunity [38–40], and the insoluble fraction of tumor cell homogenates in PBS lysed by sonication contain tumor antigens eliciting cytotoxic T-lymphocytes [41]. The method of extracting denatured proteins in high yield established in this study may therefore be useful for preparation of cancer vaccines.

Acknowledgments

The authors would like to thank emeritus professor Hidenori Yamada for many helpful discussions.

Author Contributions

Conceived and designed the experiments: JF YA KK. Performed the experiments: JF HF RK TH HT YA. Analyzed the data: RK HN HM. Contributed to the writing of the manuscript: JF RK HN.

References

1. Pace CN, Treviño S, Prabhakaran E, Scholtz JM (2004) Protein structure, stability and solubility in water and other solvents. Philos Trans R Soc Lond B Biol Sci 359: 1225–1234; discussion 1234–1225.
2. Zeskind BJ, Jordan CD, Timp W, Trapani L, Waller G, et al. (2007) Nucleic acid and protein mass mapping by live-cell deep-ultraviolet microscopy. Nat Methods 4: 567–569.
3. Guigas G, Kalla C, Weiss M (2007) Probing the nanoscale viscoelasticity of intracellular fluids in living cells. Biophys J 93: 316–323.
4. Szasz CS, Alexa A, Toth K, Rakacs M, Langowski J, et al. (2011) Protein disorder prevails under crowded conditions. Biochemistry 50: 5834–5844.
5. Tompa P (2005) The interplay between structure and function in intrinsically unstructured proteins. FEBS Lett 579: 3346–3354.
6. Song J (2009) Insight into "insoluble proteins" with pure water. FEBS Lett 583: 953–959.
7. Song J (2013) Why do proteins aggregate? "Intrinsically insoluble proteins" and "dark mediators" revealed by studies on "insoluble proteins" solubilized in pure water. F1000Res 2: 94.
8. Dunker AK, Obradovic Z, Romero P, Garner EC, Brown CJ (2000) Intrinsic protein disorder in complete genomes. Genome Inform Ser Workshop Genome Inform 11: 161–171.
9. Romero P, Obradovic Z, Kissinger CR, Villafranca JE, Garner E, et al. (1998) Thousands of proteins likely to have long disordered regions. Pac Symp Biocomput: 437–448.
10. Ward JJ, Sodhi JS, McGuffin LJ, Buxton BF, Jones DT (2004) Prediction and functional analysis of native disorder in proteins from the three kingdoms of life. J Mol Biol 337: 635–645.
11. Fukuchi S, Hosoda K, Homma K, Gojobori T, Nishikawa K (2011) Binary classification of protein molecules into intrinsically disordered and ordered segments. BMC Struct Biol 11: 29.
12. Kim TD, Ryu HJ, Cho HI, Yang CH, Kim J (2000) Thermal behavior of proteins: heat-resistant proteins and their heat-induced secondary structural changes. Biochemistry 39: 14839–14846.
13. Csizmók V, Szollosi E, Friedrich P, Tompa P (2006) A novel two-dimensional electrophoresis technique for the identification of intrinsically unstructured proteins. Mol Cell Proteomics 5: 265–273.
14. Galea CA, Pagala VR, Obenauer JC, Park CG, Slaughter CA, et al. (2006) Proteomic studies of the intrinsically unstructured mammalian proteome. J Proteome Res 5: 2839–2848.
15. Futami J, Tsushima Y, Tada H, Seno M, Yamada H (2000) Convenient and efficient in vitro folding of disulfide-containing globular protein from crude bacterial inclusion bodies. Journal of Biochemistry 127: 435–441.

16. Yamaguchi S, Yamamoto E, Mannen T, Nagamune T (2013) Protein refolding using chemical refolding additives. Biotechnol J 8: 17–31.
17. Yamada H, Seno M, Kobayashi A, Moriyama T, Kosaka M, et al. (1994) An S-alkylating reagent with positive charges as an efficient solubilizer of denatured disulfide-containing proteins. J Biochem 116: 852–857.
18. Obita T, Ueda T, Imoto T (2003) Solution structure and activity of mouse lysozyme M. Cell Mol Life Sci 60: 176–184.
19. Mishima T, Ohkuri T, Monji A, Kanemaru T, Abe Y, et al. (2010) Effects of His mutations on the fibrillation of amyloidogenic Vlambda6 protein Wil under acidic and physiological conditions. Biochem Biophys Res Commun 391: 615–620.
20. Atkinson A, Jack GW (1973) Precipitation of nucleic acids with polyethyleneimine and the chromatography of nucleic acids and proteins on immobilised polyethyleneimine. Biochim Biophys Acta 308: 41–52.
21. Chomczynski P (1993) A reagent for the single-step simultaneous isolation of RNA, DNA and proteins from cell and tissue samples. Biotechniques 15: 532–534, 536–537.
22. Hummon AB, Lim SR, Difilippantonio MJ, Ried T (2007) Isolation and solubilization of proteins after TRIzol extraction of RNA and DNA from patient material following prolonged storage. Biotechniques 42: 467–470, 472.
23. Kirkland PA, Busby J, Stevens S, Maupin-Furlow JA (2006) Trizol-based method for sample preparation and isoelectric focusing of halophilic proteins. Anal Biochem 351: 254–259.
24. Ham BM, Yang F, Jayachandran H, Jaitly N, Monroe ME, et al. (2008) The influence of sample preparation and replicate analyses on HeLa Cell phosphoproteome coverage. J Proteome Res 7: 2215–2221.
25. Gao Y, Thomas JO, Chow RL, Lee GH, Cowan NJ (1992) A cytoplasmic chaperonin that catalyzes beta-actin folding. Cell 69: 1043–1050.
26. Abe M, Abe Y, Ohkuri T, Mishima T, Monji A, et al. (2013) Mechanism for retardation of amyloid fibril formation by sugars in Vλ6 protein. Protein Sci 22: 467–474.
27. Tompa P, Dosztanyi Z, Simon I (2006) Prevalent structural disorder in E. coli and S. cerevisiae proteomes. J Proteome Res 5: 1996–2000.
28. Li M, Liu J, Song J (2006) Nogo goes in the pure water: solution structure of Nogo-60 and design of the structured and buffer-soluble Nogo-54 for enhancing CNS regeneration. Protein Sci 15: 1835–1841.
29. Li M, Liu J, Ran X, Fang M, Shi J, et al. (2006) Resurrecting abandoned proteins with pure water: CD and NMR studies of protein fragments solubilized in salt-free water. Biophys J 91: 4201–4209.
30. Yoshimura Y, Lin Y, Yagi H, Lee YH, Kitayama H, et al. (2012) Distinguishing crystal-like amyloid fibrils and glass-like amorphous aggregates from their kinetics of formation. Proc Natl Acad Sci U S A 109: 14446–14451.
31. Liu J, Song J (2009) Insights into protein aggregation by NMR characterization of insoluble SH3 mutants solubilized in salt-free water. PLoS One 4: e7805.
32. De Simone A, Kitchen C, Kwan AH, Sunde M, Dobson CM, et al. (2012) Intrinsic disorder modulates protein self-assembly and aggregation. Proc Natl Acad Sci U S A 109: 6951–6956.
33. Hoh JH (1998) Functional protein domains from the thermally driven motion of polypeptide chains: a proposal. Proteins 32: 223–228.
34. Graña-Montes R, Marinelli P, Reverter D, Ventura S (2014) N-terminal protein tails act as aggregation protective entropic bristles: the SUMO case. Biomacromolecules 15: 1194–1203.
35. Santner AA, Croy CH, Vasanwala FH, Uversky VN, Van YY, et al. (2012) Sweeping away protein aggregation with entropic bristles: intrinsically disordered protein fusions enhance soluble expression. Biochemistry 51: 7250–7262.
36. Futami J, Kitazoe M, Murata H, Yamada H (2007) Exploiting protein cationization techniques in future drug development. Expert Opinion on Drug Discovery 2: 261–269.
37. Murata H, Sakaguchi M, Futami J, Kitazoe M, Maeda T, et al. (2006) Denatured and reversibly cationized p53 readily enters cells and simultaneously folds to the functional protein in the cells. Biochemistry 45: 6124–6132.
38. Wolfraim LA, Takahara M, Viley AM, Shivakumar R, Nieda M, et al. (2013) Clinical scale electroloading of mature dendritic cells with melanoma whole tumor cell lysate is superior to conventional lysate co-incubation in triggering robust in vitro expansion of functional antigen-specific CTL. Int Immunopharmacol 15: 488–497.
39. Thumann P, Moc I, Humrich J, Berger TG, Schultz ES, et al. (2003) Antigen loading of dendritic cells with whole tumor cell preparations. J Immunol Methods 277: 1–16.
40. May M, Brookman-May S, Hoschke B, Gilfrich C, Kendel F, et al. (2010) Ten-year survival analysis for renal carcinoma patients treated with an autologous tumour lysate vaccine in an adjuvant setting. Cancer Immunol Immunother 59: 687–695.
41. Kuwada E, Kambara K, Tadaki T, Noguchi K (2011) Insoluble fraction of tumor cell homogenate is a useful material for eliciting cytotoxic T lymphocytes: a unique method for protein solubilization. Anticancer Res 31: 881–891.

VOLUME 32 · NUMBER 11 · APRIL 10 2014

JOURNAL OF CLINICAL ONCOLOGY

ORIGINAL REPORT

Multicenter Phase II Study of Mogamulizumab (KW-0761), a Defucosylated Anti-CC Chemokine Receptor 4 Antibody, in Patients With Relapsed Peripheral T-Cell Lymphoma and Cutaneous T-Cell Lymphoma

Michinori Ogura, Takashi Ishida, Kiyohiko Hatake, Masafumi Taniwaki, Kiyoshi Ando, Kensei Tobinai, Katsuya Fujimoto, Kazuhito Yamamoto, Toshihiro Miyamoto, Naokuni Uike, Mitsune Tanimoto, Kunihiro Tsukasaki, Kenichi Ishizawa, Junji Suzumiya, Hiroshi Inagaki, Kazuo Tamura, Shiro Akinaga, Masao Tomonaga, and Ryuzo Ueda

Michinori Ogura, Nagoya Daini Red Cross Hospital; Takashi Ishida and Hiroshi Inagaki, Nagoya City University Graduate School of Medical Sciences; Kazuhito Yamamoto, Aichi Cancer Center; Ryuzo Ueda, Aichi Medical University School of Medicine, Nagoya; Kiyohiko Hatake, Japanese Foundation for Cancer Research; Kensei Tobinai, National Cancer Center Hospital; Shiro Akinaga, Kyowa Hakko Kirin, Tokyo; Masafumi Taniwaki, Kyoto Prefectural University of Medicine, Kyoto; Kiyoshi Ando, Tokai University School of Medicine, Kanagawa; Katsuya Fujimoto, Hokkaido University Graduate School of Medicine, Sapporo; Toshihiro Miyamoto, Kyushu University Graduate School of Medical Sciences; Naokuni Uike, National Hospital Organization Kyushu Cancer Center; Kazuo Tamura, Fukuoka University, Fukuoka; Mitsune Tanimoto, Okayama University Hospital, Okayama; Kunihiro Tsukasaki, Nagasaki University Graduate School of Biomedical Science; Masao Tomonaga, Japanese Red Cross Nagasaki Atomic Bomb Hospital, Nagasaki; Kenichi Ishizawa, Tohoku University Hospital, Sendai; and Junji Suzumiya, Shimane University Hospital, Izumo, Japan.

Published online ahead of print at www.jco.org on March 10, 2014.

Both M.O. and T.I. contributed equally to this work.

Authors' disclosures of potential conflicts of interest and author contributions are found at the end of this article.

Clinical trial information: NCT01192984.

Corresponding author: Michinori Ogura, MD, PhD, Department of Hematology and Oncology, Nagoya Daini Red Cross Hospital, 2-9 Myoken-cho, Showa-ku, Nagoya 466-8650, Japan; e-mail: mi-ogura@naa.att.ne.jp.

0732-183X/14/3211w-1157w/$20.00

DOI: 10.1200/JCO.2013.52.0924

ABSTRACT

Purpose
CC chemokine receptor 4 (CCR4) is expressed by peripheral T-cell lymphomas (PTCLs) and is associated with poor outcomes. Mogamulizumab (KW-0761) is a defucosylated humanized anti-CCR4 antibody engineered to exert potent antibody-dependent cellular cytotoxicity. This multicenter phase II study evaluated the efficacy and safety of mogamulizumab in patients with relapsed PTCL and cutaneous T-cell lymphoma (CTCL).

Patients and Methods
Mogamulizumab (1.0 mg/kg) was administered intravenously once per week for 8 weeks to patients with relapsed CCR4-positive PTCL or CTCL. The primary end point was the overall response rate, and the secondary end points included safety, progression-free survival (PFS), and overall survival (OS).

Results
A total of 38 patients were enrolled, and 37 patients received mogamulizumab. Objective responses were noted for 13 of 37 patients (35%; 95% CI, 20% to 53%), including five patients (14%) with complete response. The median PFS was 3.0 months (95% CI, 1.6 to 4.9 months), and the median OS was not calculated. The mean maximum and trough mogamulizumab concentrations (± standard deviation) after the eighth infusion were 45.9 ± 9.3 and 29.0 ± 13.3 μg/mL, respectively. The most common adverse events were hematologic events, pyrexia, and skin disorders, all of which were reversible and manageable.

Conclusion
Mogamulizumab exhibited clinically meaningful antitumor activity in patients with relapsed PTCL and CTCL, with an acceptable toxicity profile. Further investigation of mogamulizumab for treatment of T-cell lymphoma is warranted.

J Clin Oncol 32:1157-1163. © 2014 by American Society of Clinical Oncology

INTRODUCTION

Mature T/natural killer (NK)-cell neoplasms comprise approximately 20 subclassified heterogeneous groups of non-Hodgkin lymphomas (NHLs) that account for approximately 10% of NHLs in Western countries[1-3] and approximately 25% of NHLs in Japan.[4,5] Mature T/NK-cell neoplasms are largely subdivided into peripheral T-cell lymphoma (PTCL) and cutaneous T-cell lymphoma (CTCL), and different treatment strategies are used for each of these entities.[1,6]

According to the WHO classification, PTCL includes peripheral T-cell lymphoma not otherwise specified (PTCL-NOS), angioimmunoblastic T-cell lymphoma (AITL), and anaplastic large-cell lymphoma (ALCL).[1-3] Cyclophosphamide, doxorubicin, vincristine, and prednisone (CHOP) and CHOP-like regimens have been widely used as the standard first-line treatment for patients with PTCL.[7,8] With the exception of those patients with anaplastic lymphoma kinase-positive ALCL, the efficacy of these combination therapies is unsatisfactory because those who achieve remission eventually experience relapse and poor outcomes.[3,9] Several agents have been approved by the US Food and Drug Administration for the treatment of relapsed or refractory (Rel/Ref) PTCL: pralatrexate, romidepsin for Rel/Ref PTCL, and brentuximab vedotin for Rel/Ref ALCL. The overall response rates

(ORRs) were reported to be 29% and 25% for PTCL and 86% for ALCL, respectively.[10-12]

CTCL can be classified as mycosis fungoides (MF), Sézary syndrome, or cutaneous ALCL. The majority of cases of CTCL in Japan consist of MF.[13] The therapeutic approaches and outcomes for these conditions are primarily dependent on disease stage.[6,7,14] Patients with advanced stage CTCL who relapse after systemic chemotherapies and those with transformed MF have particularly poor outcomes.[15,16] Recently, the US Food and Drug Administration approved agents for Rel/Ref CTCL treatment, including vorinostat, denileukin diftitox, and romidepsin, with ORRs of 30%, 30%, and 34%, respectively.[17-19] However, there are few treatment options or approved agents for CTCL in Japan, partly because of its low prevalence here.[5,12,13]

CC chemokine receptor 4 (CCR4) is a marker for type 2 helper T cells or regulatory T (Treg) cells and is expressed on tumor cells in approximately 30% to 65% of patients with PTCL.[20,21] CCR4-positive patients (eg, in the PTCL-NOS subgroup) have a shorter survival time when compared with CCR4-negative patients.[21-23] Further, CCR4 expression increases with advancing disease stage in patients with MF/Sézary syndrome.[24]

Mogamulizumab (KW-0761) is a humanized anti-CCR4 monoclonal antibody with a defucosylated Fc region that enhances antibody-dependent cellular cytotoxicity.[25,26] In vitro antibody-dependent cellular cytotoxicity assay and in vivo studies in a humanized mouse model revealed that mogamulizumab exhibited potent antitumor activity against T-cell lymphoma cell lines and against primary CTCL cells from patients.[26-28]

In a phase I study of patients with relapsed adult T-cell leukemia-lymphoma (ATL) and PTCL/CTCL, mogamulizumab was well tolerated up to a dose of 1.0 mg/kg. An ORR of 31% (five of 16) was obtained, including one partial response (PR) among three patients with PTCL/CTCL.[29] Mogamulizumab yielded an ORR of 50% (13 of 26) for relapsed CCR4-positive ATL in a subsequent phase II study.[30] In the United States, a phase I/II study for patients with Rel/Ref CTCL revealed that mogamulizumab was well tolerated with an ORR of 37% (14 of 38, 8% complete response [CR], 29% PR) and a median PFS of 341 days.[31]

The present report describes the results of a multicenter phase II study in Japan that was designed to assess the efficacy and safety of mogamulizumab in patients with relapsed CCR4-positive PTCL or CTCL.

PATIENTS AND METHODS

Study Design and Treatment

This was a multicenter, single-arm phase II study conducted at 15 Japanese centers. At least 35 patients were required to detect a lower limit of the 95% CI that exceeded the 5% threshold, and the expected ORR for mogamulizumab was 25% with a statistical power of 90%.[10,29]

All patients gave written informed consent before enrollment. Patients received intravenous infusions of 1.0 mg/kg mogamulizumab once per week for 8 weeks. Dose modification of mogamulizumab was not allowed. Oral antihistamine and acetaminophen were given before each dose of mogamulizumab as premedication.[29,30] A systemic corticosteroid (hydrocortisone 100 mg intravenously) was also administered before the first dose of mogamulizumab to prevent an infusion reaction. The same dose of hydrocortisone was administered before the second and subsequent administrations at the investigators' discretion. The plasma concentrations of mogamulizumab and antimogamulizumab antibodies in plasma were determined by using enzyme-linked immunosorbent assays.[29,30] Blood samples were collected from all patients who received at least one dose of mogamulizumab at times determined by the protocol for pharmacokinetic analyses. Maximum plasma mogamulizumab concentration and trough concentration parameters were calculated from 0 to 7 days after the eight doses. T-cell subsets and NK cell distribution were also investigated by flow cytometry during and after mogamulizumab treatment. This study was conducted in accordance with the Declaration of Helsinki and in compliance with Good Clinical Practices. The protocol was approved by the institutional review board at each participating institution.

Patients

Patients who were ≥ 20 years of age and who had CCR4-positive PTCL or CTCL with relapse after their last systemic chemotherapy were eligible for participation. Patients who were refractory to their most recent therapy were not eligible for this study. Histopathological subtypes were assessed and reclassified by the Independent Pathology Review Committee according to the 2008 WHO classification.[1] CCR4 expression was determined by immunohistochemistry by using an anti-CCR4 monoclonal antibody (KM2160) and was confirmed by central review, as described previously.[29] In brief, CCR4 expression was classified according to the proportion of stained tumor cells (negative, < 10%; 1+, 10% to <25%; 2+, 25% to < 50%; 3+, ≥ 50%). Staging of nodal/extranodal and/or cutaneous lesions was performed if the lesions met the following requirements: nodal and extranodal lesions were > 1.5 cm in measurable length on cross-sectional computed tomography images, cutaneous lesions were identifiable on visual inspection, and peripheral blood abnormal lymphocyte count was ≥ 1,000/μL and comprised ≥ 5% of total leukocytes. All patients were required to have an Eastern Cooperative Oncology Group performance status of 0 to 2. Other notable eligibility criteria regarding laboratory values were as follows: neutrophil count ≥ 1,500/μL, platelet count ≥ 50,000/μL, hemoglobin level ≥ 8.0 g/dL, AST level ≤ 2.5× the upper limit of normal (ULN), ALT level ≤ 2.5× the ULN, total bilirubin level ≤ 1.5× the ULN, and serum creatinine level ≤ 1.5× the ULN. Patients were excluded if they had any severe complications, such as CNS involvement or a bulky lymphoma mass requiring emergent radiotherapy, a history of allogeneic stem-cell transplantation, active concurrent cancers, an active infection, or positivity for hepatitis B virus DNA, hepatitis B surface antigen, hepatitis C virus antibody, or human immunodeficiency virus antibody.

Efficacy and Safety Assessment

The primary objective was to assess the best overall response, and the secondary objectives included assessments of the best response according to disease site, progression-free survival (PFS), and overall survival (OS). Efficacy was evaluated by the Independent Efficacy Assessment Committee according to modified response criteria based on the International Working Group Criteria.[32,33] Cutaneous lesions were evaluated by using the modified Severity Weighted Assessment Tool.[34] In addition, treatment efficacy in patients with CTCL was evaluated by using a Global Response Score.[35] Responses were assessed after the fourth and eighth mogamulizumab infusions and at 2 and 4 months after the end of treatment. Treatment was discontinued if progressive disease (PD) was evident. PD and survival were monitored until at least 4 months after the completion of dosing. For safety evaluations, adverse events (AEs) were graded according to the National Cancer Institute Common Terminology Criteria for AEs, version 4.0.

Statistical Analysis

PFS and OS were analyzed by using the Kaplan-Meier method. PFS was defined as the time from the first dose of mogamulizumab to progression, relapse, or death by any cause (whichever occurred first). OS was measured from the day of the first dose to death by any cause.

RESULTS

Patient Characteristics

Sixty-five patients were screened, and 64 biopsy specimens were histologically confirmed as PTCL or CTCL by the Independent Pathology Review Committee. In total, 50 (78%) of the 64 screened

patients were CCR4-positive. Of these, 38 eligible patients were enrolled in the study and 37 received at least one infusion of mogamulizumab. One patient withdrew because of an infectious complication before dosing. Patient characteristics, histopathology subtypes, and previous systemic therapies are shown in Table 1.

Table 1. Baseline Patient Demographic and Clinical Characteristics

Characteristic*	Patients (N = 37) No.	%	Patients With PTCL (n = 29) No.	%	Patients With CTCL (n = 8) No.	%
Age, years						
Median	64		67		50	
Range	33-80		33-80		36-70	
≥ 65	18	49	17	59	1	13
Sex						
Male	23	62	20	69	3	38
Female	14	38	9	31	5	63
ECOG performance status						
0	24	65	19	66	5	63
1	12	32	10	34	2	25
2	1	3	0	0	1	13
Elevated LDH level†	21	57	18	62	3	38
Bone marrow involvement	7	19	7	24	0	0
No. of previous systemic regimens						
Median	2		2		3	
Range	1-6		1-5		1-6	
1	14	38	13	45	1	13
2	15	41	12	41	3	38
≥ 3	8	22	4	14	4	50
Types of systemic therapy						
Chemotherapy	37	100	29	100	8	100
CHOP/CHOP-like regimen	36	97	29	100	7	88
DeVIC	6	16	4	14	2	25
CHASE	5	14	5	17	0	0
Single-agent therapy	5	14	0	0	5	63
Other	10	27	10	34	0	0
Auto-PBSCT	3	8	3	10	0	0
Radiotherapy	9	24	5	17	4	50
Intensity of CCR4 expression‡						
1+	6	16	4	14	2	25
2+	6	16	4	14	2	25
3+	25	68	21	72	4	50
Histopathology by central review						
PTCL-NOS	16	43	16	55		
AITL	12	32	12	41		
ALCL, ALK negative	1	3	1	4		
MF	7	19			7	88
c-ALCL	1	3			1	13

Abbreviations: AITL, angioimmunoblastic T-cell lymphoma; ALCL, anaplastic large-cell lymphoma; ALK, anaplastic lymphoma kinase; c-ALCL, cutaneous anaplastic large-cell lymphoma; CHASE, cyclophosphamide, cytosine arabinoside, etoposide, and dexamethasone; CHOP, cyclophosphamide, doxorubicin, vincristine, and prednisone; CTCL, cutaneous T-cell lymphoma; DeVIC, dexamethasone, etoposide, ifosfamide, and carboplatin; ECOG, Eastern Cooperative Oncology Group; LDH, lactate dehydrogenase; MF, mycosis fungoides; NOS, not otherwise specified; PBSCT, peripheral-blood stem-cell transplantation; PTCL, peripheral T-cell lymphoma.

*Of the 38 patients enrolled, 37 received at least one infusion of mogamulizumab.

†Elevated LDH level: higher LDH level than upper limit of the normal range.

‡The denominator used for the intensity of CC chemokine receptor 4 (CCR4) expression is based on subjects who were positive for CCR4 by immunohistochemistry.

Of the 37 patients who received mogamulizumab, 25 (68%) completed the planned course of eight infusions. Nine patients (24%) discontinued treatment because of PD, and three patients (8%) due to serious AEs.

Efficacy

The ORR for the 37 treated patients was 35% (13 of 37; 95% CI, 20% to 53%), and 14% of patients (five of 37) achieved a CR, of which one was unconfirmed (Table 2). Reponses (CR/PR) were observed in at least one patient with each subtype of disease, but the ORR differed between subtypes. The ORR was 34% (10 of 29; 95% CI, 18% to 54%) in patients with PTCL (three of 16 for PTCL-NOS, six of 12 for AITL, and one of one for ALCL, anaplastic lymphoma kinase-negative) and 38% (three of eight; 95% CI, 9% to 76%) in those with CTCL (two of seven for MF and one of one for cutaneous ALCL). In addition, ORR in patients with CTCL was 50% (four of eight; 95% CI, 16% to 84%) according to the Global Response Score.

Total ORR did not significantly correlate with CCR4 expression level, patient age, or the number of previous chemotherapy regimens. The response rates for lymph node and cutaneous lesions were 33% (11 of 33) and 58% (seven of 12), respectively.

The median PFS was 3.0 months (95% CI, 1.6 to 4.9 months) for the entire population and 2.0 months for patients with PTCL. Although the median OS was not reached for the entire population at the

Table 2. Best Response (N = 37)

Parameter	No. of Patients	No. of Patients With Best Response CR/CRu	PR	SD	PD	Response Rate (%)*
Overall response	37	5	8	13	11	35
Histopathology by central review						
PTCL	29	5†	5	9	10	34
PTCL-NOS	16	1	2	6	7	19
AITL	12	3	3	3	3	50
ALCL, ALK negative	1	1†	0	0	0	100
CTCL	8	0	3	4	1	38
MF	7	0	2	4	1	29
c-ALCL	1	0	1	0	0	100
Age, years						
< 65	19	1†	6	7	5	37
≥ 65	18	4	2	6	6	33
Intensity of CCR4 expression						
1+	6	1	1	3	1	33
2+	6	1	2	2	1	50
3+	25	3†	5	8	9	32
No. of previous systemic regimens						
1	14	3	3	6	2	43
2	15	1	1	6	7	13
≥ 3	8	1†	4	1	2	63

Abbreviations: AITL, angioimmunoblastic T-cell lymphoma; ALCL, anaplastic large-cell lymphoma; ALK, anaplastic lymphoma kinase; c-ALCL, cutaneous anaplastic large-cell lymphoma; CCR4, CC chemokine receptor 4; CR, complete response/complete remission; CRu, uncertain complete response/uncertain complete remission; CTCL, cutaneous T-cell lymphoma; MF, mycosis fungoides; NOS, not otherwise specified; PD, progressive disease; PR, partial response/partial remission; PTCL, peripheral T-cell lymphoma; SD, stable disease.

*Response rate (%): 100 × number of responders/number of subjects in each category included in the efficacy analysis set.

†Among the patients who showed CR/CRu, one showed CRu.

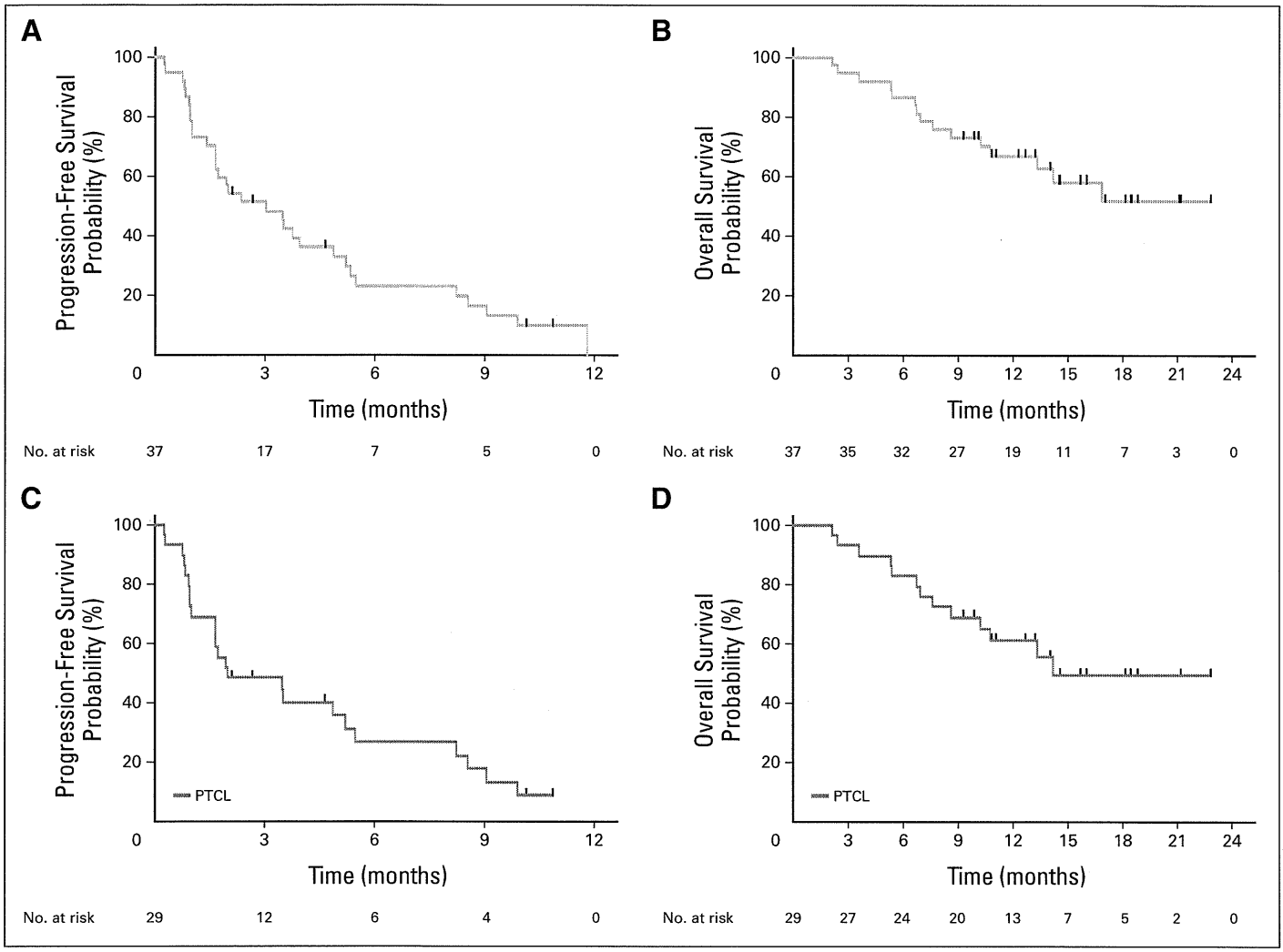

Fig 1. Kaplan-Meier curves of (A) estimated progression-free survival (median, 3.0 months), (B) overall survival (median not reached), (C) progression-free survival in patients with peripheral T-cell lymphoma (PTCL; median, 2.0 months), and (D) overall survival in patients with PTCL (median, 14.2 months).

time of this report, it was 14.2 months for patients with PTCL (Fig 1). Moreover, the median PFS of all 13 responders was 5.5 months, and for PTCL responders (n = 10), it was 8.2 months.

Safety

The most common treatment-related AEs of all grades and treatment-related AEs of grade 3/4 were lymphocytopenia (81%, 73%), neutropenia (38%, 19%), and leukocytopenia (43%, 14%), whereas the most common nonhematologic AE was pyrexia (30%; grade 2 or lower) (Table 3). Lymphocytopenia occurred in 30 patients (81%) and was noted after the first dose in 26 of these patients. For 19 of the patients, lymphocyte counts were $< 800/\mu L$ (grades 2 to 4) before the first dosing. The lymphocyte count ultimately recovered to normal or baseline levels in all patients.

Infusion reaction (24%; grade 2 or lower) occurred primarily at the first infusion, after which it became less frequent, and all patients recovered. No infusion prolongation/interruption was caused by the infusion reaction.

In addition, treatment-related skin disorders were commonly reported (all grades, 51%; grade 3/4, 11%) when grouped according to system organ class. Of the 19 patients who suffered from skin disorder complications, 15 patients experienced improvement, whereas the remaining patients discontinued treatment because of PD or switched to other post treatments. One patient who had a history of psoriasis before the study treatment developed two serious skin disorders (toxicoderma and psoriasis vulgaris) during the study period.

Fifteen serious treatment-related AEs were observed among eight patients (22%); these AEs included grade 3 polymyositis in one patient, grade 2 cytomegalovirus retinitis in two patients, and grade 4 second primary malignancy in one patient with AITL. All patients improved over time, and there were no deaths related to AEs.

Pharmacokinetics and Pharmacodynamics

The mean maximum mogamulizumab concentration and trough mogamulizumab concentration ($\pm$ standard deviation) in plasma after the eighth infusion were 45.9 $\pm$ 9.3 and 29.0 $\pm$ 13.3 μg/mL, respectively. Antimogamulizumab antibodies were not detected after dosing in any patients. These results were consistent with the findings of a previous study of patients with ATL.[30] As an exploratory study, we assessed the effect of mogamulizumab on the number of CD4+/CD25+/Foxp3+ cells (the Treg cell subset) and CD45+/CD16+/CD56+ cells (the NK cell subset). Patients given

